

# A MAC Throughput in the Wireless LAN

Ha Cheol Lee

*Dept. of Information and Telecom. Eng., Yuhan University, Bucheon City,  
Korea*

## 1. Introduction

Over the past few years, mobile networks have emerged as a promising approach for future mobile IP applications. With limited frequency resources, designing an effective MAC (Medium Access Control) protocol is a hot challenge. IEEE 802.11b/g/a/n networks are currently the most popular wireless LAN products on the market [1]. The conventional IEEE 802.11b and 802.11g/a specification provide up to 11 and 54 Mbps data rates, respectively. However, the MAC protocol that they are based upon is the same and employs a CSMA/CA (Carrier Sense Multiple Access/Collision Avoidance) protocol with binary exponential back-off. IEEE 802.11 DCF (Distributed Coordination Function) is the de facto MAC protocol for wireless LAN because of its simplicity and robustness [2,3]. Therefore, considerable research efforts have been put on the investigation of the DCF performance over wireless LAN [2]. With the successful deployment of IEEE 802.11a/b/g wireless LAN and the increasing demand for real-time applications over wireless, the IEEE 802.11n Working Group standardized a new MAC and PHY (Physical) layer specification to increase the bit rate to be up to 600 Mbps [3]. The throughput performance at the MAC layer can be improved by aggregating several frames before transmission [3]. Frame aggregation not only reduces the transmission time for preamble and frame headers, but also reduces the waiting time during CSMA/CA random backoff period for successive frame transmissions. The frame aggregation can be performed within different sub-layers. In 802.11n, frame aggregation can be performed either by A-MPDU (MAC Protocol Data Unit Aggregation) or A-MSDU (MAC Service Data Unit Aggregation). Although frame aggregation can increase the throughput at the MAC layer under ideal channel conditions, a larger aggregated frame will cause each station to wait longer before its next chance for channel access. Under error-prone channels, corrupting a large aggregated frame may waste a long period of channel time and lead to a lower MAC efficiency [4]. On the other hand, wireless LAN mobile stations that are defined as the stations that access the LAN while in motion are considered in this chapter. The previous paper analyzed the IEEE 802.11b/g/n MAC performance for wireless LAN with fixed stations, not for wireless LAN with mobile stations [5, 6, 7, 8, 9, 10]. On the contrary, Xi Yong [11] and Ha Cheol Lee [12] analyzed the MAC performance for IEEE 802.11 wireless LAN with mobile stations, but considered only IEEE 802.11 and 802.11g/a wireless LAN specification. So, this chapter summarizes all the reference papers and analyzes the IEEE 802.11b/g/a/n MAC performance for wireless LAN with fixed and mobile stations. In other words, we will present the analytical evaluation of saturation

throughput with bit errors appearing in the transmitting channel. In Section 2, wireless LAN history and standards are reviewed. In section 3, wireless LAN access network is reviewed. IEEE 802.11b/g/a/n/ac/ad PHY and MAC layer are reviewed in Section 4. In Section 5, frame error rate of wireless channel and the DCF saturation throughput are theoretically derived. Finally, it is concluded with Section 6.

## 2. Wireless LAN history and standards

Standards in the IEEE project 802 target the PHY layer and MAC layer. When wireless LAN was first conceived, it seemed that it would be just another PHY of one of the available standards. The first candidate considered for this was IEEE's most prominent standard 802.3 (Ethernet). However, it soon became obvious that the radio medium is very different from the well-behaved wire. Due to tremendous attenuation even over short distances, collisions cannot be detected. Hence, 802.3's CSMA/CD (Carrier Sense Multiple Access/Collision Detection) could not be applied. The next candidate standard to be considered was 802.4. Its coordinated medium access, the token bus concept, was believed to be superior to 802.3's contention-based scheme. Hence, WLAN began as 802.4L. However, already in 1990 it was obvious that token handling in radio networks was difficult. The standardization body realized that a wireless communication standard would need its own very unique MAC. Finally, on March 21, 1991, project 802.11 was approved. The first 802.11 standard was published in 1997. At the PHY layer it provides three solutions: a FHSS (Frequency Hopping Spread Spectrum) and a DSSS (Direct Sequence Spread Spectrum) PHY in the unlicensed 2.4 GHz band, and an infrared PHY at 316–353 THz. Although all three provide a basic data rate of 1 Mb/s with an optional 2 Mb/s mode, commercial infrared implementations do not exist. Similar to 802.3, basic 802.11 MAC operates according to a listen-before-talk scheme, and is known as the DCF. It implements CSMA/CA rather than collision detection as in 802.3. Indeed, as collision cannot be detected in the radio environment, 802.11 waits for a backoff interval before each frame transmission rather than after collisions. In addition to DCF, the original 802.11 standard specifies an optional scheme that depends on a central coordination entity, the PCF (Point Coordination Function). This function uses the so called PC (Point Coordinator) that operates during the so-called contention-free period. The latter is a periodic interval during which only the PC initiates frame exchanges via polling. However, the PCF's poor robustness against hidden nodes resulted in negligible adoption by manufacturers. Having published its first 802.11 standard in 1997, the WG (Working Group) received feedback that many products did not provide the degree of compatibility customers expected. As an example, often the default encryption scheme, called WEP (Wired Equivalent Privacy), would not work between devices of different vendors. This need for a certification program led to the foundation of the WECA (Wireless Ethernet Compatibility Alliance) in 1999, renamed the WFA (Wi-Fi Alliance) in 2003. Wi-Fi certification has become a well-known certification program that has significant market impact. The tremendous success in the market and the perceived shortcomings of the base 802.11 standard provided a basis and impetus for a prolific program of improvements and extensions. This has led to revisions of the draft, driven by a complete alphabet of amendments. It is the purpose of this article to review this process and explain both the contents of these amendments and their interrelation. In the following we first describe the changes made to the PHY layer and then turn to the improvements to the MAC layer. In both, we make a distinction between what has already been accepted and what is currently in the process of being standardized [2].

Standard	Spectrum	Maximum physical rate	Layer 2 data rate	Tx	Compatible with	Major disadvantage	Major advantage
802.11n	2.4/5 GHz	600 Mbps	100 Mbps	MIMO OFDM	802.11b/g/a	Difficult to implement	Highest bit rate
802.11b	2.4 GHz	11 Mbps	6-7 Mbps	DSSS	802.11	Bit rate too low for many emerging applications	Widely deployed, higher range
802.11g	2.4 GHz	54 Mbps	32 Mbps	OFDM	802.11/802.11b	Limited number of collocated WLANs	Higher bit rate in 2.4 GHz spectrum
802.11a	5.0 GHz	54 Mbps	32 Mbps	OFDM	None	Smallest range of all 802.11 standards	Higher bit rate in less-crowded spectrum

Table 1. Wireless LAN products on the market [1]

### 2.1 PHY related amendments

Although not interoperable, the DSSS and FHSS PHY initially seemed to have equal chances in the market. The FHSS PHY even had a duplicate in the HomeRF group that aimed at integrated voice and data services. This used plain 802.11 with FHSS for data transfer, complemented with a protocol for voice that was very similar to the Digital Enhanced Cordless Telecommunications standard. Neither HomeRF nor 802.11 saw FHSS extensions, although plans for a second-generation HomeRF existed that targeted at 10 Mb/s. In contrast, the high-rate project 802.11b was started in December 1997 and boosted the data rates of the DSSS PHY to 11 Mb/s. This caused 802.11b to ultimately supersede FHSS, including HomeRF, in the market. Figure 1 provides an overview of the 802.11 PHY amendments and their dependencies [2].

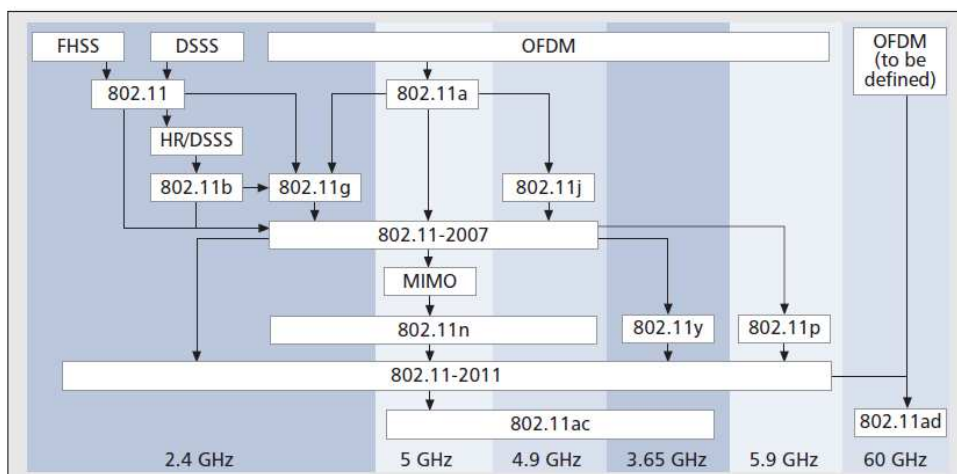


Fig. 1. The 802.11 PHY layer amendments and their dependencies [2]

### 2.1.1 802.11a/g

The first extension project, 802.11a, started in September 1997. It added an OFDM (Orthogonal Frequency Division Multiplexing) PHY that supports up to 54 Mb/s data rate. Since 802.11a operates in the 5 GHz band, communication with plain 802.11 devices is impossible. This lack of interoperability led to the formation of 802.11g, which introduced the benefits of OFDM to the 2.4 GHz band. As 802.11g's extended rate PHY provides DSSS-compatible signaling, an easy migration from 802.11 to 802.11g devices became possible. During the standardization process, a single manufacturer already sold pre-802.11g chipsets. With its proprietary PBCC (Packet Binary Convolutional Code), additional data rates of 22 Mb/s and 33 Mb/s were supported. Today rarely applied, PBCC set a de facto standard and became an optional MCS (Modulation and Coding Scheme) of 802.11g. To comply with the European regulatory requirements for the 5 GHz band, 802.11h was introduced at the end of 2003. While in the United States the FCC describes absolute radio output power limits, in Europe antenna gain must not be used for transmission. Furthermore, satellite uplink and radar stations must be secured from interference. Therefore, 802.11h defines MAC mechanisms for DFS (Dynamic Frequency Selection) and TPC (Transmit Power Control), which we explain in the MAC section. Ratified in 2004, 802.11j describes the necessary means to comply with Japanese regulatory requirements for the operation of 802.11 equipment in the 4.9 GHz and 5 GHz frequency bands. Besides requirements on medium access discussed in the next section, 802.11j is the first amendment that defines PHY operation with 10 MHz bandwidth in addition to the formerly preferred 20 MHz channelization.

Data Rate (Mbits/sec)	Modulation	Coding Rate (R)	Coding Bits Per Subcarrier ( $N_{BPSK}$ )	Coded Bits per OFDM symbol ( $N_{CBPS}$ )	Data Bits Per OFDM Symbol ( $N_{DBPS}$ )
6	BPSK	1/2	1	48	24
9	BPSK	3/4	1	48	36
12	QPSK	1/2	2	96	48
18	QPSK	3/4	2	96	72
24	16-QAM	1/2	4	192	96
36	16-QAM	3/4	4	192	144
48	64-QAM	2/3	6	288	192
54	64-QAM	3/4	6	288	216

Table 2. Parameters of the IEEE 802.11a physical layer

While IEEE 802.11b uses only DSSS technology, IEEE 802.11g uses DSSS, OFDM, or both at the 2.4 GHz ISM band to provide high data rates of up to 54 Mb/s. Combined use of both

DSSS and OFDM is achieved through the provision of four different physical layers. These layers, defined in the standard as ERPs (Extended Rate Physicals), coexist during a frame exchange, so the sender and receiver have the option to select and use one of the four layers as long as they both support it. The four different physical layers defined in the IEEE 802.11g standard are the following :

- *ERP-DSSS/CCK*: This is the old physical layer used by IEEE 802.11b. DSSS technology is used with CCK modulation. The data rates provided are those of IEEE 802.11b.
- *ERP-OFDM*: This is a new physical layer, introduced by IEEE 802.11g. OFDM is used to provide IEEE 802.11a data rates at the 2.4 GHz band.
- *ERP-DSSS/PBCC*: This physical layer was introduced in IEEE 802.11b and provides the same data rates as the DSSS/CCK physical layer. It uses DSSS technology with the PBCC coding algorithm. IEEE 802.11g extended the set of data rates by adding those of 22 and 33 Mb/s.
- *DSSS-OFDM*: This is a new physical layer that uses a hybrid combination of DSSS and OFDM. The packet physical header is transmitted using DSSS, while the packet payload is transmitted using OFDM. The scope of this hybrid approach is to cover interoperability aspects, as explained later. From the above four physical layers, the first two are mandatory; every IEEE 802.11g device must support them. The other two are optional. Column 2 of Table 3 summarizes the supported data rates for the different physical layers of the IEEE 802.11g specification.

Physical layer	Supported rates (Mb/s)	PLCP preamble + header delay		PLCP preamble + header length	
		Long	Short	Long	Short
ERP-DSSS (mandatory)	1, 2, 5.5, 11	192 $\mu$ s	96 $\mu$ s	192 bits	120 bits
ERP-OFDM (mandatory)	6, 9, 12, 18, 24, 36, 48, 54	20 $\mu$ s		40 bits	
ERP-PBCC (optional)	1, 2, 5.5, 11, 22, 33	192 $\mu$ s	96 $\mu$ s	192 bits	120 bits
DSSS-OFDM (optional)	6, 9, 12, 18, 24, 36, 48, 54	192 $\mu$ s	96 $\mu$ s	192 bits	120 bits

Table 3. Parameters of the different IEEE 802.11g physical layers [8]

### 2.1.2 802.11n

As the first project whose targeted data rate is measured on top of the MAC layer, 802.11n provides user experiences comparable to the well known Fast Ethernet (802.3u). Far beyond the minimum requirements that were derived from its wired paragon's maximum data rate of 100 Mb/s, 802.11n delivers up to 600 Mb/s. Its most prominent feature is MIMO capability. A flexible MIMO (Multiple Input Multiple Output) concept allows for arrays of up to four antennas that enable spatial multiplexing or beam forming. Its most debated innovation is the usage of optional 40 MHz channels. Although this feature was already

being used as a proprietary extension to 802.11a and 802.11g chipsets, it caused an extensive discussion on neighbor friendly behavior. Especially for the 2.4 GHz band, concerns were raised that 40 MHz operation would severely affect the performance of existing 802.11, Bluetooth (802.15.1), ZigBee (802.15.4), and other devices. The development of a compromise, which disallows 40 MHz channelization for devices that cannot detect 20 MHz-only devices, prevented ratification of 802.11n until September 2009. As a consequence of 20/40 MHz operation and various antenna configurations, 802.11n defines a total of 76 different MCSs. Since several of them provide similar data rates, WFA's certification program decides the MCSs finally used in the market. 802.11n's PHY enhancements are supported by medium access enhancements we introduce in the MAC section.

MCS Index	Modulation	Coding Rate	Spatial Streams	802.11n Data Rate (Mbps)			
				20-MHz		40-MHz	
				L-GI	S-GI	L-GI	S-GI
0	BPSK	1/2	1	6.5	7.2	13.5	15
1	QPSK	1/2	1	13	14.4	27	30
2	QPSK	3/4	1	19.5	21.7	40.5	45
3	16-QAM	1/2	1	26	28.9	54	60
4	16-QAM	3/4	1	39	43.3	81	90
5	64-QAM	2/3	1	52	57.8	108	120
6	64-QAM	3/4	1	58.5	65	122	135
7	64-QAM	5/6	1	65	72.2	135	150
8	BPSK	1/2	2	13	14.4	27	30
9	QPSK	1/2	2	26	28.9	54	60
10	QPSK	3/4	2	39	43.3	81	90
11	16-QAM	1/2	2	52	57.8	108	120
12	16-QAM	3/4	2	78	86.7	162	180
13	64-QAM	2/3	2	104	116	216	240
14	64-QAM	3/4	2	117	130	243	270
15	64-QAM	5/6	2	130	144	270	300
16	BPSK	1/2	3	19.5	21.7	40.5	45
17	QPSK	1/2	3	39	43.3	81	90
18	QPSK	3/4	3	58.5	65	121.5	135
19	16-QAM	1/2	3	78	86.7	162	180
20	16-QAM	3/4	3	117	130	243	270
21	64-QAM	2/3	3	156	173.3	324	360
22	64-QAM	3/4	3	175.5	195	364.5	405
23	64-QAM	5/6	3	195	216.7	405	450
24	BPSK	1/2	4	26	28.9	54	60
25	QPSK	1/2	4	52	57.8	108	120
26	QPSK	1/2	4	78	86.7	162	180
27	16-QAM	1/2	4	104	115.6	216	240
28	16-QAM	3/4	4	156	173.3	324	360
29	64-QAM	2/3	4	208	231.1	432	480
30	64-QAM	3/4	4	234	260	486	540
31	64-QAM	5/6	4	260	288.9	540	600

Table 4. Parameters of the IEEE 802.11n physical layer, MCS Rates 0-31 [13]

### 2.1.3 802.11ac/ad

802.11ac and 802.11ad develop amendments that fulfill the ITU's (International Telecommunication Union's) requirements on proposals for the IMT Advanced standard. Both target greater than 1 Gb/s throughput, but while 802.11ac considers the traditional Wireless LAN frequencies below 6 GHz, 802.11ad competes with the Wireless Personal Area Network TG (Task Group) 802.15.3c, standard ECMA 387, and the Wireless Gigabit Alliance on the 60 GHz frequency spectrum. Due to their premature stage, both TGs are still in the process of collecting input and specific proposals from their members. At the moment of writing this article, 802.11ad has already started defining some additional requirements regarding range (at least 10 m at 1 Gb/s), seamless session transfer of an active session from the 60 GHz band to the 2.4/5 GHz band and vice versa, coexistence with other systems in the band such as 802.15.3c, and support for uncompressed video requirements such as data rate, packet loss ratio, and delay.

## 2.2 MAC related amendments

A key element to the 802.11 success is its simple MAC operation based on the DCF protocol. This scheme has proven to be robust and adaptive to varying conditions, able to cover most needs sufficiently well. Following the trends visible from the wired Ethernet, 802.11's success is mainly based on overprovisioning of its capacity. The available data rate was sufficient to cover the original best effort applications, so complex resource scheduling and management algorithms were unnecessary. However, this may change in the future. Because of the growing popularity of 802.11, WLANs are expected to reach their capacity limits. Moreover, applications like voice and video streaming pose different demands for quality of service. Therefore, traffic differentiation and network management might become inevitable. In the following we explain 802.11 MAC related extensions of the amendments introduced in the previous section and those shown in Fig. 2 [2].

### 2.2.1 802.11e

The original project goal of 802.11e, approved at the end of March 2000, foresaw general enhancements of the WLAN standard. Efficiency improvements, support for quality of service (QoS), and security enhancements were its key elements. However, already in 2001, the 802.11 frame encryption algorithm WEP was broken by an attack. Thus, security enhancements were displaced to a new TG called 802.11i. After intensive discussions, 802.11e was finally approved in 2005 to support QoS. As a new medium access scheme, 802.11e provides the HCF (Hybrid Coordination Function), where *hybrid* relates to HCF's two MAC protocol versions with centralized and distributed control, respectively. The first is implemented by HCF HCCA (HCF Controlled Channel Access), an improved variant of the PCF requiring a central coordination instance that schedules medium access. Until today no device implementing HCCA is known to exist in the market. EDCA is HCF's second MAC protocol. While DCF does not differentiate between traffic with different QoS needs, EDCA (Enhanced Distributed Channel Access) provides support for four traffic categories: voice, video, best effort, and background with different rules to access the wireless medium. Accordingly, EDCA enables service differentiation. Both centralized and distributed MAC protocols change the medium sharing rules. Without 802.11e, a WLAN provides per packet fairness: regardless of the actual frame transmission duration, devices back off after every single frame. In contrast, duration of all

HCCA and EDCA frame exchanges is bound by the TXOP (Transmission Opportunity) limit. Thus, devices share time slices of the wireless medium. Those that use faster MCSs may exchange multiple frames after a single successful contention and consequently achieve higher throughput. Derived from EDCA, WFA has successfully branded and introduced to the market an EDCA variant called WMM (Wi-Fi MultiMedia). WMM incorporates a subset of functions from 802.11e draft 6 (November 2003). As the final 802.11e and WMM specifications differ, some members of the 802.11 initiated a QoS Enhancement SG (Study Group) in May 2007. Its intended goal was an adaptation of the 802.11e amendment to the WMM specification. However, a project could never be approved, and the SG was dissolved in November 2007.

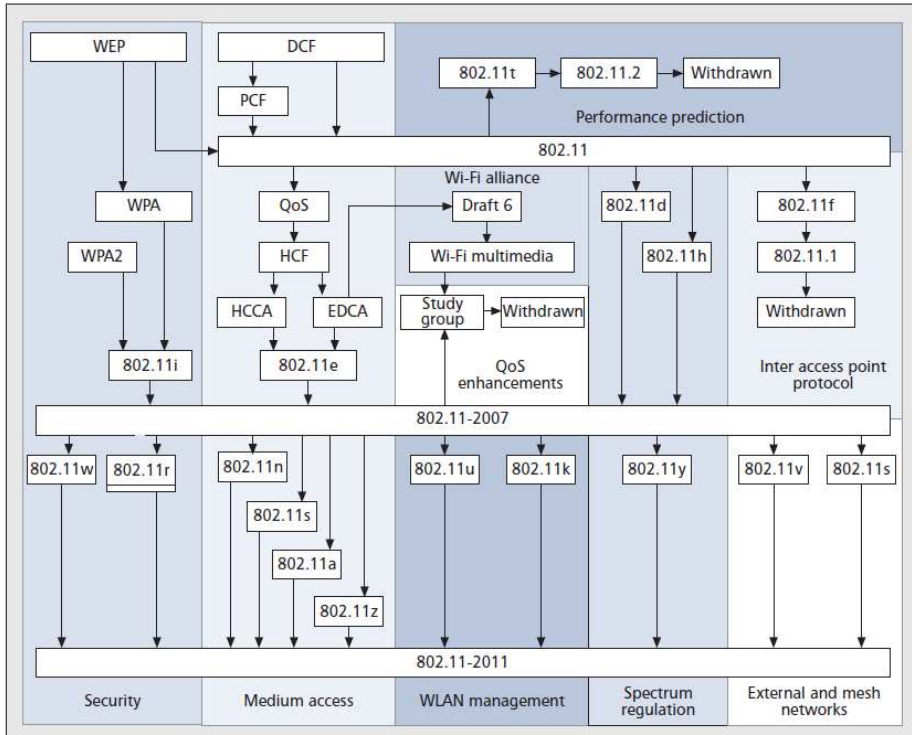


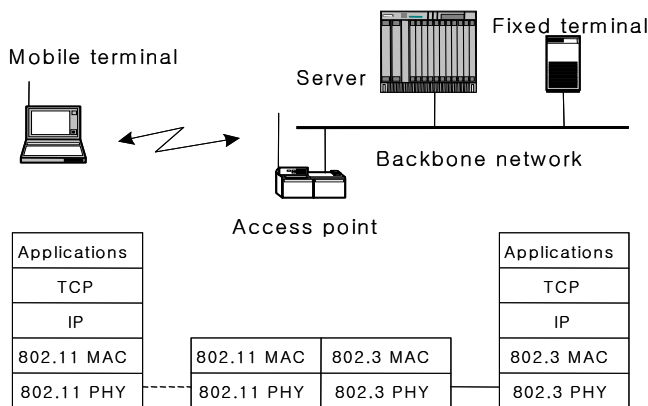
Fig. 2. The 802.11 MAC layer amendments [2]

### 3. Wireless LAN access network

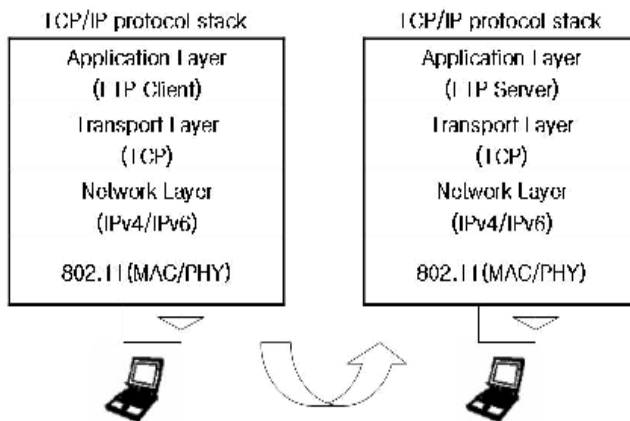
This section shows infrastructure-based and ad hoc-based operation of wireless access architecture in the 802.11b/a/g/n-based mobile LAN. The protocols of the various layers are called the protocol stack. The TCP/IP protocol stack consists of five layers: the physical, data link, network, transport and application layers. This section is focused on physical layer and data link layer which consists of MAC and LLC (Logical Link Control) sub-layers. An ad hoc network might be formed when people with laptops get together and want to exchange data in the absence of a centralized AP (Access Point). Wireless LAN topology is ad hoc-based or infrastructure-based as shown in Fig. 3. The ad hoc-based topology shows



that each user in the wireless network communicates directly with all others without a backbone network. Infrastructure-based topology shows that all wireless users transmit to an AP to communicate with users on the wired or wireless LAN. IEEE 802.11 operates in the 2.4 GHz band and supports data rates 1 Mbps to 2 Mbps. IEEE 802.11b uses DSSS (Direct Sequence Spread Spectrum) but supports data rates of up to 11 Mbps. The modulation scheme employed is called CCK (Complementary Code Keying). The operating frequency range is 2.4 GHz and hence can interfere with some home appliances. IEEE 802.11g achieves very high data rates compared to IEEE 802.11b and uses the 2.4 GHz frequency band. An IEEE 802.11b client can operate with an 802.11g AP. IEEE 802.11a equipment is more expensive and consumes more power, as it uses OFDM (Orthogonal Frequency Division Multiplexing). OFDM uses 12 orthogonal channels in the 5 GHz range. The frequency channels are nonoverlapping. The achievable data rates are 6, 9, 12, 18, 24, 36, 48 and 54 Mbps. IEEE 802.11a and 802.11b can operate next to each other without any interference. Fig. 4 shows the IEEE 802.11b/a/g/n-based physical and MAC layer protocol stack.



(a) Infrastructure-based wireless LAN



(b) Ad-hoc mode operation in the wireless LAN

Fig. 3. Protocol stack in the IEEE 802.11 wireless LAN [12]

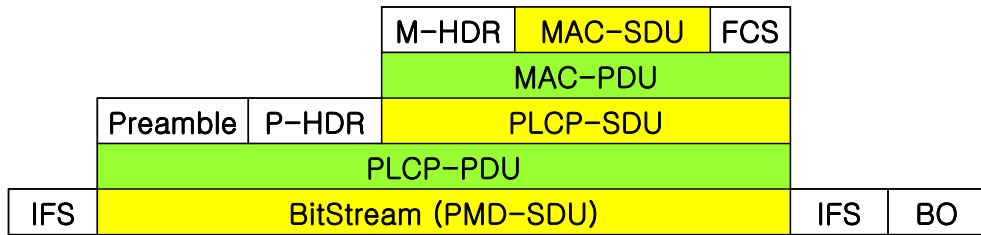


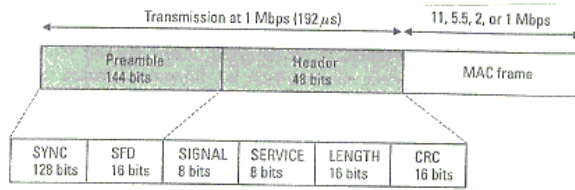
Fig. 4. Protocol stack of physical and MAC layer [12]

IEEE 802.11 protocol stack consists of MAC layer and PHY layer. When a network layer pushes a user packet down to the MAC layer as a MAC-SDU (MAC-Service Data Unit), overheads are added to the MAC layer and MAC-PDU (MAC-Protocol Data Unit) is created. The PHY layer is divided into a PLCP (Physical Layer Convergence Protocol) sublayer and a PMD (Physical Medium Dependent) sublayer. In this PHY layer, the same procedure as MAC layer is also executed. IEEE 802.11 MAC layer uses an 802.11 PHY layer, such as 802.11a/b/g, to perform the tasks such as carrier sensing, transmission, and reception of 802.11 frames. With regards to the MAC layer, the functional specifications are essentially the same for all of them with minor differences.

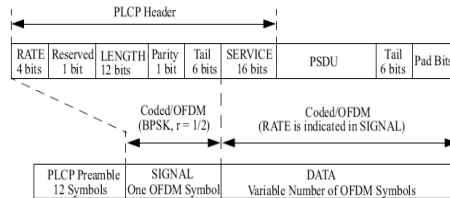
## 4. Wireless LAN PHY/MAC layer

### 4.1 IEEE 802.11b/a/g PHY/MAC layer

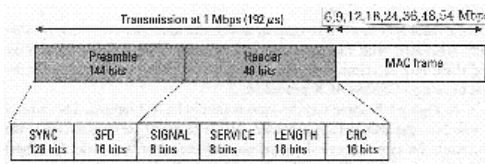
When a higher layer pushes a user packet down to the MAC layer as a MAC-SDU, the MAC layer header (M-HDR) and trailer (FCS) are added before and after the MSDU, respectively and form a MAC-PDU. The PHY layer is again divided into a PLCP sub-layer and a PMD sub-layer. Similarly the PLCP preamble and PLCP header (P-HDR) are attached to the MPDU at the PLCP sub-layer. Different IFS (Inter Frame Space)s are added depending on the type of MPDU. IEEE 802.11a operates in the 5 GHz band and uses OFDM. The achievable data rates are 6, 9, 12, 18, 24, 36, 48, and 54 Mbps. 802.11g uses DSSS, OFDM, or both at the 2.4 GHz ISM band to provide high data rates of up to 54 Mbps. 802.11g device can operate with an 802.11b device. Combined use of both DSSS and OFDM is achieved through the provision of four different physical layers. The four different physical layers defined in the 802.11g standards are ERP-DSSS/CCK, ERP-OFDM, ERP-DSSS/PBCC and DSSS-OFDM. The standards that support the highest data rate of 54 Mbps are ERP-OFDM and DSSS-OFDM. ERP-OFDM is a new physical layer in IEEE 802.11g and OFDM is used to provide IEEE 802.11a data rates at the 2.4 GHz band. DSSS-OFDM is a new physical layer that uses a hybrid combination of DSSS and OFDM. The packet physical header is transmitted using DSSS, while the packet payload is transmitted using OFDM. Basic access scheme is CSMA/CA mechanism. The SIFS (Short Inter-Frame Space) and the slot time are determined by the physical layer. DIFS (Distributed Inter-Frame Space) is defined based on the above two intervals.



(a) 802.11b ERP-OFDM frame



(b) 802.11a and 802.11g ERP-OFDM frame



(c) 802.11g DSSS-OFDM frame

Fig. 5. Frame structure of IEEE 802.11b/a/g-based wireless LAN [12]

IEEE 802.11 MAC protocol supports the DCF and the PCF . The DCF uses the CSMA/CA mechanism for contention-based access, while the PCF provides contention-free access. The two modes are used alternately in time. IEEE 802.11 MAC protocol defines five timing intervals. Two of them are the SIFS and the slot time that are determined by the physical layer. The other three intervals are the PIFS (Priority InterFrame Space), DIFS and EIFS (Extended InterFrame Space) that are defined based on the above two intervals. But the PCF is restricted to infrastructure network configurations. Therefore, the DCF is widely assumed under the consideration of ad hoc-based wireless LAN. Fig. 6 shows two access schemes. IEEE 802.11 DCF stations access the channel via a basic access method or the four-way handshaking access method with an additional RTS/CTS message exchange. In the basic access method, the CSMA mechanism is applied. Stations wait for the channel to be idle for a DIFS period of time and then execute backoff for data transmission. Stations choose a random number between 0 and CW (Contention Window)-1 with equal probability as a backoff timer. When the backoff timer reaches zero, the data frame is transmitted. The receiver replies an ACK message upon successfully receiving a data packet. In the four-way handshaking access method, when the backoff timer of station reaches zero, the station first transmits a RTS frame. Upon receiving the RTS frame, the receiver replies with a CTS frame after a SIFS period. Once the RTS/CTS is exchanged successfully, the sender then transmits its data frame. The RTS and CTS frames carry a duration field, information of time interval to transmit the

packet. Any station receiving RTS or CTS frames can read the duration field information. That information is then used to update a NAV (Network Allocation Vector) value that indicates to each station the amount of time that remains before the channel will become idle. Therefore, a station detecting the RTS and CTS frames suitably delays further transmission, and thus avoids collision. The NAV is thus referred to as a virtual carrier sensing mechanism. The main purpose of the RTS/CTS handshaking is to resolve the so-called hidden node problem.

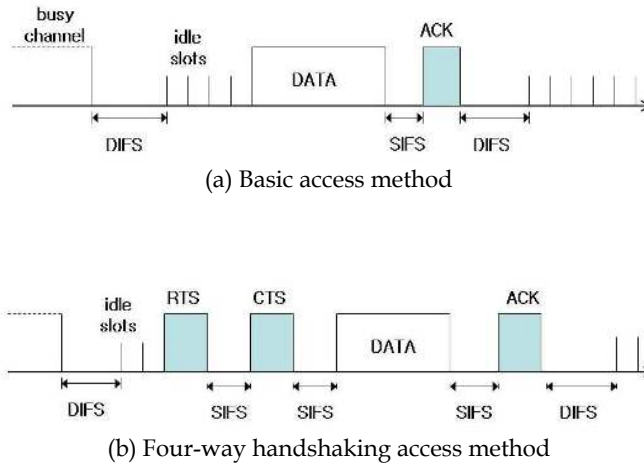


Fig. 6. IEEE 802.11 DCF channel access mechanism [14]

Parameter	802.11b	802.11g	802.11a
$T_{slot}$	20 $\mu$ s	9 $\mu$ s/20 $\mu$ s	9 $\mu$ s
T	1 $\mu$ s	1 $\mu$ s	1 $\mu$ s
$T_P$	144 $\mu$ s	16 $\mu$ s/144 $\mu$ s	16 $\mu$ s
$CW_{min}$	31	31/15	15
$T_{PHY}$	48 $\mu$ s	4 $\mu$ s/48 $\mu$ s	4 $\mu$ s
$T_{SYM}$	N/A	N/A, 4 $\mu$ s	4 $\mu$ s
$T_{DIFS}$	50 $\mu$ s	50 $\mu$ s/34 $\mu$ s	34 $\mu$ s
$T_{SIFS}$	10 $\mu$ s	16 $\mu$ s	16 $\mu$ s

Table 5. Parameters of IEEE 802.11b/g/a [6, 7, 8]

MAC scheme	Transmission	T <sub>DIFS</sub>	T <sub>SIFS</sub>	T <sub>BO</sub>	T <sub>RTS</sub>	T <sub>CTS</sub>	T <sub>ACK</sub>	T <sub>DATA</sub> (MSDU : bytes)
CSMA/CA	DSSS-1	50	10	310	N/A	N/A	304	192+8×(34+MSDU)/1
	DSSS-2	50	10	310	N/A	N/A	304	192+8×(34+MSDU)/2
	HR-5.5	50	10	310	N/A	N/A	304	192+8×(34+MSDU)/5.5
	HR-11	50	10	310	N/A	N/A	304	192+8×(34+MSDU)/11
	OFDM-6	34	9	67.5	N/A	N/A	44	20+4×[(16+6+8×(34+MSDU))/24]
	OFDM-12	34	9	67.5	N/A	N/A	32	20+4×[(16+6+8×(34+MSDU))/48]
	OFDM-24	34	9	67.5	N/A	N/A	28	20+4×[(16+6+8×(34+MSDU))/96]
	OFDM-54	34	9	67.5	N/A	N/A	24	20+4×[(16+6+8×(34+MSDU))/216]
RTS/CTS	DSSS-1	50	10×3	310	352	304	304	192+8×(34+MSDU)/1
	DSSS-2	50	10×3	310	352	304	304	192+8×(34+MSDU)/2
	HR-5.5	50	10×3	310	352	304	304	192+8×(34+MSDU)/5.5
	HR-11	50	10×3	310	352	304	304	192+8×(34+MSDU)/11
	OFDM-6	34	9×3	67.5	52	44	44	20+4×[(16+6+8×(34+MSDU))/24]
	OFDM-12	34	9×3	67.5	36	32	32	20+4×[(16+6+8×(34+MSDU))/48]
	OFDM-24	34	9×3	67.5	28	28	28	20+4×[(16+6+8×(34+MSDU))/96]
	OFDM-54	34	9×3	67.5	24	24	24	20+4×[(16+6+8×(34+MSDU))/216]

Table 6. Delay compents for different MAC schemes (unit :  $\mu$ s) [7]

#### 4.2 IEEE 802.11n PHY/MAC layer

The key requirement that drove most of the development in 802.11n is the capability of at least 100 Mb/s MAC throughput. Considering that the typical throughput of 802.11a/g is 25 Mb/s (with a 54 Mb/s PHY data rate), this requirement dictated at least a fourfold increase in throughput. Defining the requirement as MAC throughput rather than PHY data rate forced developers to consider the difficult problem of improving MAC efficiency. The inability to achieve a throughput of 100 Mb/s necessitated substantial improvements in MAC efficiency when designing the 802.11n MAC. Two basic concepts are employed in 802.11n to increase the PHY data rates: MIMO and 40 MHz bandwidth channels. Increasing from a single spatial stream and one transmit antenna to four spatial streams and four antennas increases the data rate by a factor of four. The term *spatial stream* is defined in the 802.11n standard as one of several bitstreams that are transmitted over multiple spatial dimensions created by the use of multiple antennas at both ends of a communications link. However, due to the inherent increased cost associated with increasing the number of antennas, modes that use three and four spatial streams are optional. And to allow for handheld devices, the two spatial streams mode is only mandatory in an AP. 40 MHz bandwidth channel operation is optional in the standard due to concerns regarding interoperability between 20 and 40 MHz bandwidth devices, the permissibility of the use of 40 MHz bandwidth channels in the various regulatory domains, and spectral efficiency. However, the 40 MHz bandwidth channel mode has become a core feature due to the low cost of doubling the data rate from doubling the bandwidth. Almost all 802.11n products on the market feature a 40 MHz mode of operation. Other minor modifications were also made to the 802.11a/g waveform to

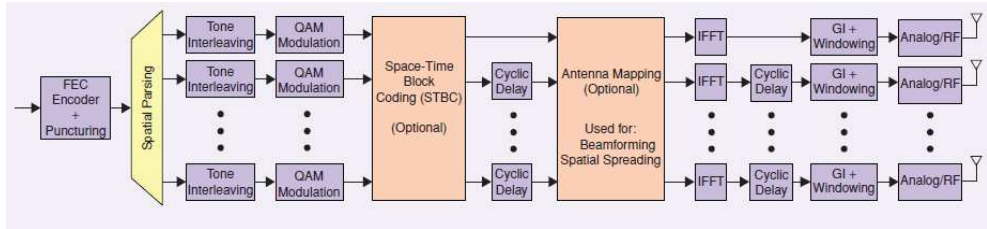
increase the data rate. The highest encoder rate in 802.11a/g is  $3/4$ . This was increased to  $5/6$  in 802.11n for an 11 percent increase in data rate. With the improvement in RF (Radio Frequency) technology, it was demonstrated that two extra frequency subcarriers could be squeezed into the guard band on each side of the spectral waveform and still meet the transmit spectral mask. This increased the data rate by 8 percent over 802.11a/g. Lastly, the waveform in 802.11a/g and mandatory operation in 802.11n contains an 800 ns guard interval between each OFDM symbol. An optional mode was defined with a 400 ns guard interval between each OFDM symbol to increase the data rates by another 11 percent. Another functional requirement of 802.11n was interoperability between 802.11a/g and 802.11n. The TG decided to meet this requirement in the physical layer by defining a waveform that was backward compatible with 802.11a and OFDM modes of 802.11g. The preamble of the 802.11n mixed format waveform begins with the preamble of the 802.11a/g waveform. This includes the 802.11a/g short training field, long training field, and signal field. This allows 802.11a/g devices to detect the 802.11n mixed format packet and decode the signal field. Even though the 802.11a/g devices will not be able to decode the remainder of the 802.11n packet, they will be able to properly defer their own transmission based on the length specified in the signal field. The remainder of the 802.11n Mixed format waveform includes a second short training field, additional long training fields, and additional signal fields followed by the data. These new fields are required for MIMO training and signaling of the many new modes of operation. To ensure backward compatibility between 20 MHz bandwidth channel devices (including 802.11n and 802.11a/g) and 40 MHz bandwidth channel devices, the preamble of the 40 MHz waveform is identical to the 20 MHz waveform and is repeated on the two adjacent 20 MHz bandwidth channels that form the 40 MHz bandwidth channel. This allows 20 MHz bandwidth devices on either adjacent channel to decode the signal field and properly defer transmission. The preamble in 802.11a has a length of 20  $\mu\text{s}$ ; with the additional training and signal fields, the 802.11n mixed format packet has a preamble with a length of 36  $\mu\text{s}$  for one spatial stream up to 48  $\mu\text{s}$  for four spatial streams. Unfortunately, MIMO training and backward compatibility increases the overhead, which reduces efficiency. In environments free from legacy devices (termed *greenfield*) backward compatibility is not required.

By eliminating the components of the preamble that support backward compatibility, the greenfield format preamble is 12  $\mu\text{s}$  shorter than the mixed format preamble. This difference in efficiency becomes more pronounced when the packet length is short, as in the case of VoIP traffic. Therefore, the use of the greenfield format is permitted even in the presence of legacy devices with proper MAC protection, although the overhead of the MAC protection may reduce the efficiency gained from the PHY. Range was considered as a performance metric in the PAR and comparison criteria. To increase the data rate at a given range requires enhanced robustness of the wireless link. 802.11n defines implicit and explicit TxBF (Transmit BeamForming) methods and STBC (Space-Time Block Coding), which improves link performance over MIMO with basic SDM (Spatial-Division Multiplexing). The standard also defines a new optional LDPC (Low Density Parity Check) encoding scheme, which provides better coding performance over the basic convolutional code. To break the 100 Mb/s throughput barrier, frame aggregation was added to the 802.11n MAC as the key method of increasing efficiency. The issue is that as the data rate increases, the time on air of the data portion of the packet decreases. However, the PHY and MAC overhead remain

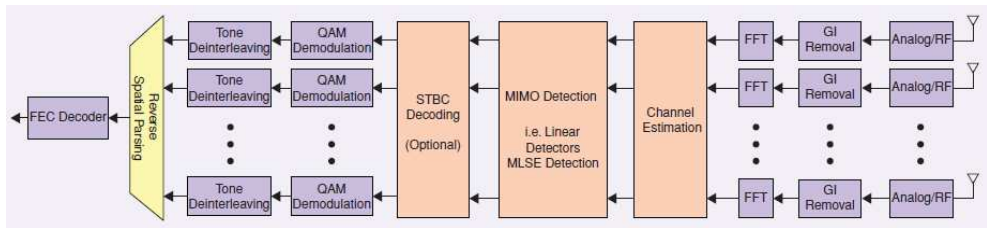
constant. This results in diminishing returns from the increase in PHY data rate. Frame aggregation increases the length of the data portion of the packet to increase overall efficiency. Two forms of aggregation exist in the standard: A-MPDU and A-MSDU. Logically, A-MSDU resides at the top of the MAC and aggregates multiple MSDUs into a single MPDU. Each MSDU is prepended with a subframe header consisting of the destination address, source address, and a length field giving the length of the SDU in bytes. This is then padded with 0 to 3 bytes to round the subframe to a 32-bit word boundary. Multiple such subframes are concatenated together to form a single MPDU. An advantage of A-MSDU is that it can be implemented in software. A-MPDU resides at the bottom of the MAC and aggregates multiple MPDUs. Each MPDU is prepended with a header consisting of a length field, 8-bit CRC, and 8-bit signature field. These subframes are similarly padded to 32-bit word boundaries. Each subframe is concatenated together. An advantage of A-MPDU is that if an individual MPDU is corrupt, the receiver can scan forward to the next MPDU by detecting the signature field in the header of the next MPDU. With A-MSDU, any bit error causes all the aggregates to fail.

Standards	802.11a/g	802.11n	
		Mandatory	Optional
Maximum transmission rate (Mbps)	54	130	600
Bandwidth(MHz)	20	20	40
FFT size	64	64	128
Number of subcarrier (data + pilot)	52 (48+4)	56 (52+4)	114 (108+6)
Multi-antenna scheme	signal antenna	2 Tx MIMO	3,4 Tx MIMO Tx Beam forming STBC
Channel coding	Convolutional code (1/2, 2/3, 3/4)	Convolutional code (1/2, 2/3, 3/4, 5/6)	LDPC (1/2, 2/3, 3/4, 5/6)
Modulation	BPSK, QPSK, 16-QAM, 64-QAM		
Spatial stream	1	1 ~ 2	1 ~ 4
Guard interval(ns)	800	800	400
Subcarrier interval	312.5 KHz	312.5 KHz	312.5 KHz
FFT period	3.2 $\mu$ s	3.2 $\mu$ s	3.2 $\mu$ s
Symbol period	4 $\mu$ s	4 $\mu$ s	4 $\mu$ s

Table 7. IEEE 802.11n OFDM parameter compared to IEEE 802.11a/g



(a) General MIMO TX Datapath



(b) General MIMO RX Datapath

Fig. 7. Block diagrams of general MIMO transmit and receive datapath structures for an IEEE 802.11n PHY [15]

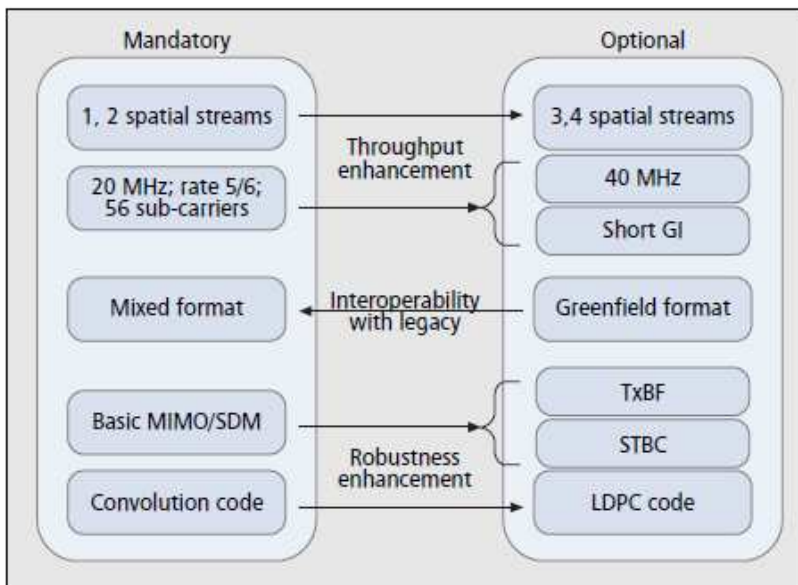


Fig. 8. Mandatory and optional 802.11n PHY features [4]



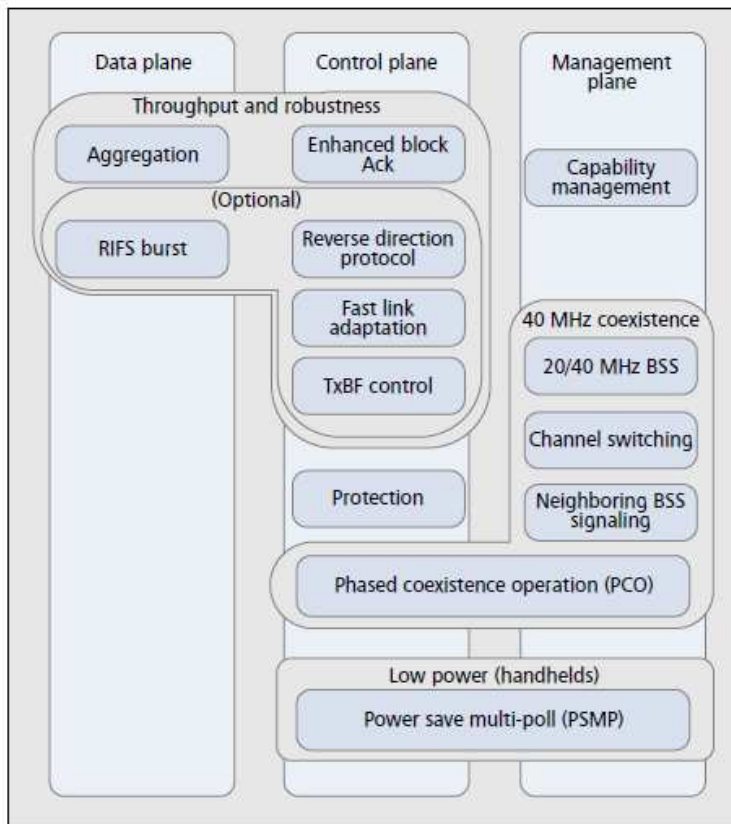


Fig. 9. Summary of 802.11n MAC enhancements [4]

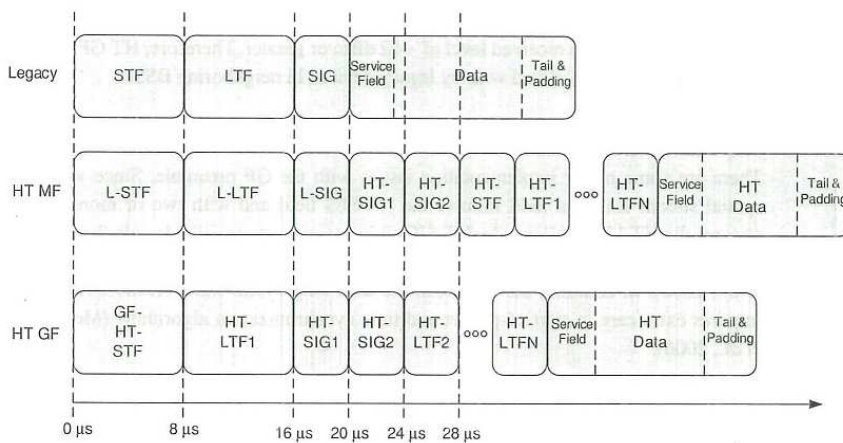


Fig. 10. Timing of the preamble fields in legacy, MF and GF in IEEE 802.11n wireless LAN[14]

The possible timing sequences for A-MPDU and A-MSDU in the uni-directional transfer case are shown in Fig. 11. If RTS/CTS (Request To Send/Clear To Send) is used, the current transmission sequence of RTS-CTS-DATA (Data frame)-ACK (Acknowledgement) only allows the sender to transmit a single data frame. The DATA frame represents either an A-MPDU or an A-MSDU frame. The system time can be broken down into virtual time slots where each slot is the time interval between two consecutive countdown of backoff timers by non-transmitting stations. The 802.11n also specifies a bi-directional data transfer method.

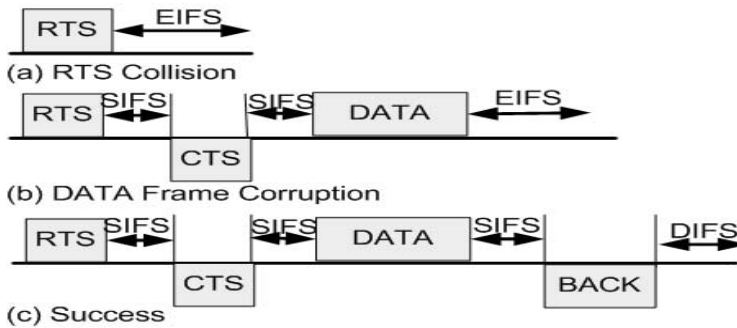


Fig. 11. IEEE 802.11n Uni-directional RTS/CTS Access Scheme [14][9]

In the bi-directional data transfer method, the receiver may request a *reverse* data transmission in the CTS control frame. The sender can then grant a certain medium time for the receiver on the reverse link. The transmission sequence will then become RTS-CTS-DATAf-DATAR-ACK. This facilitates the transmission of some small feedback packets from the receiver and may also enhance the performance of TCP (Transmission Control Protocol) which requires the transmission of TCP ACK segments. BACK (Block Acknowledgement) can be used to replace the previous ACK frame. The BACK can use a bit map to efficiently acknowledge each individual sub-frame within the aggregated frame. For the bi-directional data transfer, the reverse DATAr frame can contain a BACK to acknowledge the previous DATAf frame. In this subsection, we briefly mention the most important MAC enhancements with a more detailed explanation on frame aggregation, which maximizes throughput and efficiency. Aggregate exchange sequences are made possible with a protocol that acknowledges multiple MPDUs with a single block ACK in response to a block acknowledgment request (BAR). Another key enhancement that the 802.11n specifies is the bidirectional data transfer method over a single TXOP, known as reverse direction. This feature permits the transportation of data frames, even aggregates, in both directions in one TXOP. Until now, when the sender STA is allocated with a TXOP, it informs surrounding STAs about how long the wireless medium will be engaged. However, this approximation of channel use is not always accurate, and often the transmission ends sooner. As a result, contended STAs assume that the channel is still occupied when this is not the case. With reverse direction, the initial receiver STA is allowed to send any packets available that are addressed to the sender for the remaining TXOP time. This fits especially well with TCP because it allows a TCP link to *piggyback* TCP ACK collection onto TCP data transmission. The long-NAV (Network Allocation Vector) is another enhancement that improves scheduling, given that a station that holds a TXOP may set a longer NAV value intended to protect multiple PPDU. Another mandatory feature is PCO (Phased Coexistence

Operation) which protects stations using either 20 MHz or 40 MHz channel spectrum at the same time. Finally, the RIFS (Reduced IFS) is proposed to allow a time interval of 2  $\mu$ s between multiple PPDUs, which is much shorter than SIFS as defined in the legacy standards.

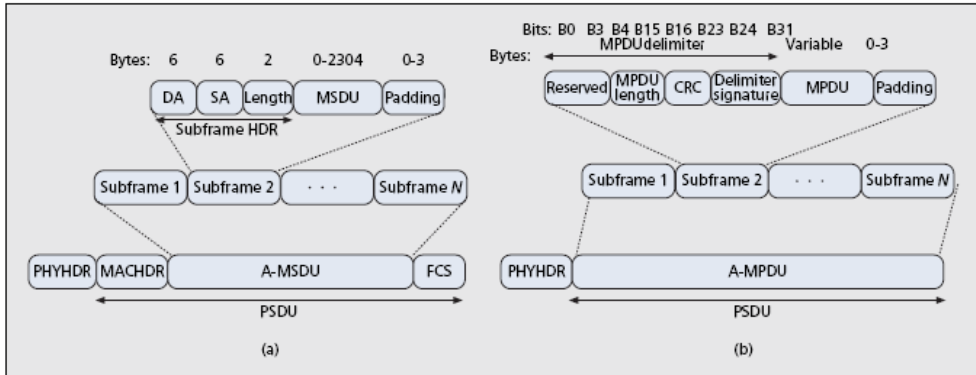


Fig. 12. One-level frame aggregation: a) A-MSDU; b) A-MPDU [10]

**A-MSDU** – The principle of the A-MSDU (or MSDU aggregation) is to allow multiple MSDUs to be sent to the same receiver concatenated in a single MPDU. This definitely improves the efficiency of the MAC layer, specifically when there are many small MSDUs, such as TCP acknowledgments. This supporting function for A-MSDU within the 802.11n is mandatory at the receiver. For an A-MSDU to be formed, a layer at the top of the MAC receives and buffers multiple packets (MSDUs). The A-MSDU is completed either when the size of the waiting packets reaches the maximal A-MSDU threshold or the maximal delay of the oldest packet reaches a pre-assigned value. Its maximum length can be either 3839 or 7935 bytes; this is 256 bytes shorter than the maximum PHY PSDU length (4095 or 8191 bytes, respectively), as predicted space is allocated for future status or control information. The size can be found in the HT capabilities element that is advertised from an HT STA in order to declare its HT status. The maximal delay can be set to an independent value for every AC but is usually set to 1  $\mu$ s for all ACs. There are also certain constraints when constructing an A-MSDU:

- All MSDUs must have the same TID value
- Lifetime of the A-MSDU should correspond to the maximum lifetime of its constituent elements
- The DA (Destination Address) and SA (Sender Address) parameter values in the subframe header must match to the same RA (Receiver Address) and TA (Transmitter Address) in the MAC header.

Thus, broadcasting or multicasting is not allowed. Figure 12a describes a simple structure of a carrier MPDU that contains an A-MSDU. Each subframe consists of a subframe header followed by the packet that arrived from the LLC and 0 ~ 3 bytes of padding. The padding size depends on the rule that each subframe, except for the last one, should be a multiple of four bytes, so the end receiver can approximate the beginning of the next subframe. A major drawback of using A-MSDU is under error-prone channels. By compressing all MSDUs into a single MPDU with a single sequence number, for any subframes that are corrupted, the

entire A-MSDU must be retransmitted. Additional frame structures or optimum frame sizes have been proposed to improve performance under noisy channels.

**A-MPDU** – The concept of A-MPDU aggregation is to join multiple MPDU subframes with a single leading PHY header. A key difference from A-MSDU aggregation is that A-MPDU functions after the MAC header encapsulation process. Consequently, the A-MSDU restriction of aggregating frames with matching TIDs is not a factor with A-MPDUs. However, all the MPDUs within an A-MPDU must be addressed to the same receiver address. Also, there is no waiting/holding time to form an A-MPDU so the number of MPDUs to be aggregated totally depends on the number of packets already in the transmission queue. The maximum length that an A-MPDU can obtain – in other words the maximum length of the PSDU that may be received – is 65,535 bytes, but it can be further constrained according to the capabilities of the STA found in the HT capabilities element. The utmost number of subframes that it can hold is 64 because a block ACK bitmap field is 128 bytes in length, where each frame is mapped using two bytes. Note that these two bytes are required to acknowledge up to 16 fragments but because A-MPDU does not allow fragmentation, these extra bits are excessive. As a result, a new variant has been implemented, known as compressed block ACK with a bitmap field of eight bytes long. Finally, the size of each subframe is limited to 4095 bytes as the length of a PPDU cannot exceed the 5.46-ms time limit; this can be derived from the maximum length divided by the lowest PHY rate, which is 6 Mb/s and is the highest duration of an MPDU in 802.11a. The basic structure is shown in Fig. 12b. A set of fields, known as delimiters are inserted before each MPDU and padding bits varied from 0 ~ 3 bytes are added at the tail. The basic operation of the delimiter header is to define the MPDU position and length inside the aggregated frame. It is noted that the CRC (Cyclic Redundancy Check) field in the delimiter verifies the authenticity of the 16 preceding bits. The padding bytes are added such that each MPDU is a multiple of four bytes in length, which can assist subframe delineation at the receiver side. In other words, the MPDU delimiters and PAD bytes determine the structure of the A-MPDU. After the AMPDU is received, a de-aggregation process initiates. First it checks the MPDU delimiter for any errors based on the CRC value. If it is correct, the MPDU is extracted, and it continues with the next subframe till it reaches the end of the PSDU. Otherwise, it checks every four bytes until it locates a valid delimiter or the end of the PSDU. The delimiter signature has a unique pattern to assist the de-aggregation process while scanning for delimiters.

### 4.3 IEEE 802.11ac/ad PHY/MAC layer

The WiGig (Wireless Gigabit) Alliance was formed to meet this need by establishing a unified specification for wireless communication at multi-gigabit speeds; this specification is designed to drive a global ecosystem of interoperable products. The WiGig MAC and PHY Specification enables data rates up to 7 Gbps, more than 10 times the speed of the fastest Wi-Fi networks based on IEEE 802.11n. It operates in the unlicensed 60 GHz frequency band, which has much more spectrum available than the 2.4 GHz and 5 GHz bands used by existing Wi-Fi products. This allows wider channels that support faster transmission speeds. The WiGig specification is based on the existing IEEE 802.11 standard, which is at the core of hundreds of millions of Wi-Fi products deployed worldwide. The specification includes native support for Wi-Fi over 60 GHz; new devices with tri-band radios will be able to seamlessly integrate into existing 2.4 GHz and 5 GHz Wi-Fi networks. The specification enables a broad range of advanced uses,

including wireless docking and connection to displays, as well as virtually instantaneous wireless backups, synchronization and file transfers between computers and handheld devices. For the first time, consumers will be able to create a complete computing and consumer electronics experience without wires. The WiGig specification includes key features to maximize performance, minimize implementation complexity and cost, enable compatibility with existing Wi-Fi and provide advanced security. Key features include:

- Support for data transmission rates up to 7 Gbps; all devices based on the WiGig specification will be capable of gigabit data transfer rates
- Designed from the ground up to support low-power handheld devices such as cell phones, as well as high-performance devices such as computers; includes advanced power management
- Based on IEEE 802.11; provides native Wi-Fi support and enables devices to transparently switch between 802.11 networks operating in any frequency band including 2.4 GHz, 5 GHz and 60 GHz
- Support for beamforming, maximizing signal strength and enabling robust communication at distances beyond 10 meters
- Advanced security using the Galois/Counter Mode of the AES encryption algorithm
- Support for high-performance wireless implementations of HDMI, DisplayPort, USB and PCIe

The WiGig specification defines PHY and MAC layers and is based on IEEE 802.11. This enables native support for IP networking over 60 GHz. It also makes it simpler and less expensive to produce devices that can communicate over both WiGig and existing Wi-Fi using tri-band radios (2.4 GHz, 5 GHz and 60 GHz).

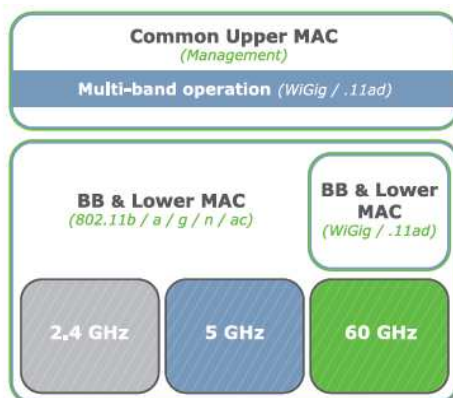


Fig. 13. WiGig architecture enables tri-band communications [16]

The WiGig Alliance is also defining PALs (Protocol Adaptation Layers) that support specific data and display standards over 60 GHz. PALs allow wireless implementations of these standard interfaces that run directly on the WiGig MAC and PHY, as shown in Figure 14, and can be implemented in hardware. The initial PALs are audio-visual (A/V), which defines support for HDMI and DisplayPort, and input-output (I/O), which defines support for USB and PCIe.

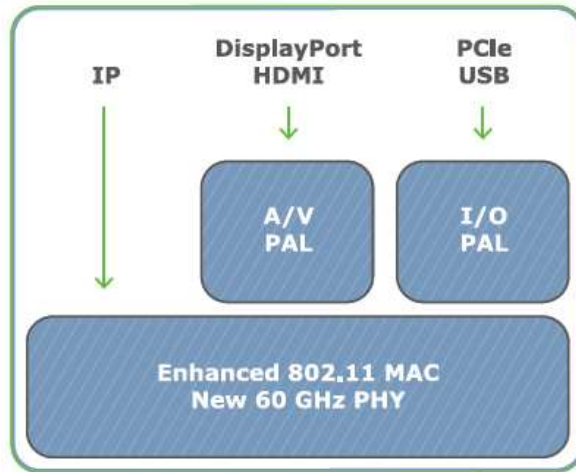


Fig. 14. WiGig Protocol Adaptation Layers (PALs) [16]

MCS	Modulation	R	N <sub>BPSK</sub>	N <sub>SD</sub>	N <sub>SP</sub>	N <sub>CBPS</sub>	N <sub>DBPS</sub>	N <sub>SS</sub>	Data rate [Mbps]	
									800 ns GI	400ns GI
1	64-QAM	2/3	6	228	8	5,472	3,648	4	912	1,013
2	64-QAM	3/4	6	228	8	5,472	4,104	4	1,026	1,140
3	64-QAM	5/6	6	228	8	5,472	4,560	4	1,140	1,266

Table 8. Transmission rate performance of IEEE 802.11ac [17]

Modulation with RS(255,233)	Data rate [Mbps]	
	Narrowband mode	Wideband mode
BPSK-1/2	162	708.6
BPSK-3/4	243	1062.9
QPSK-1/2	323	1417.2
QPSK-3/4	486	2125.7
16-QAM-1/2	647.8	2834.3
16-QAM-3/4	971.75	4251.4
64-QAM-2/3	1295.66	5668.5

Table 9. Transmission rate performance of IEEE 802.11ad [18]

Parameter	Value
FFT size	256
Number of total sub-carrier	244
Data subcarrier	228
Sub-carrier spacing	312.5 KHz
FFT period	3.2 $\mu$ s
Guard interval	800 ns, 400 ns, 200 ns
Symbol period	4 $\mu$ s

Table 10. IEEE 802.11ac OFDM parameter [17]

Parameter	Value	
	Narrowband mode	Wideband mode
Channel bandwidth	540/720 MHz	2,160 MHz
FFT bandwidth	576 MHz	2,304 MHz
FFT size	256	1,024
Sub-carrier spacing	2.25 MHz	2.25 MHz
Guard interval	111 ns	111ns
FFT period	444 ns	444 ns
OFDM symbol time	556 ns	556 ns
Data sub-carriers	192	768
Pilot/Zero sub-carriers	16/5	60/5
Nominal used bandwidth	479.25 MHz	2,049.75 MHz

Table 11. IEEE 802.11ad OFDM parameter [18]

## 5. Frame error rate and DCF throughput analysis

### 5.1 Frame error rate

#### 5.1.1 Frame error rate of fixed wireless channel

In IEEE 802.11a/g wireless LAN, fixed wireless channel is assumed to be Rayleigh fading channel. The probability of bit error is upper bound by

$$P_b < \frac{1}{k} \sum_{d=d_{free}}^{\infty} B_d P_d \tag{1}$$

where  $d_{free}$  is the free distance of the convolutional code,  $B_d$  is the total number of information bit ones on all weight  $d$  paths,  $P_d$  is the probability of selecting a weight  $d$  output sequence as the transmitted code sequence, and  $k$  is the number of information bits per clock cycle. Because the weight structure is generally accepted that the first five terms in equation (1) dominate, equation (1) can be rewritten as

$$P_b < \frac{1}{k} \sum_{d=d_{free}}^{d_{free}+4} B_d P_d \tag{2}$$

The probability of selecting the incorrect path when  $d$  is odd.

$$P_d = \sum_{i=\frac{d+1}{2}}^d \binom{d}{i} p^i (1-p)^{d-i} \tag{3}$$

where  $p$  is the probability of channel bit error. The probability of selecting the incorrect path when  $d$  is even.

$$P_d = \sum_{i=\frac{d}{2}+1}^d \binom{d}{i} p^i (1-p)^{d-i} + \frac{1}{2} \binom{d}{d/2} p^{d/2} (1-p)^{d/2} \tag{4}$$

To achieve data rates of 54 Mbps for wireless access, the IEEE 802.11a standard utilizes MQAM( $q=6, M=64$ ) with convolutional coding at rate  $r = 3/4$ . We obtain the approximate channel bit error probability for the  $i^{th}$  sub-channel for MQAM with a square constellation as [19]

$$p_i \approx \frac{4 \left(1 - \frac{1}{\sqrt{M}}\right) \cdot e^{-d \cdot \zeta_i \left[ \frac{3qr\overline{\gamma}_{b_i}}{3qr\overline{\gamma}_{b_i} + 2(M-1)(\zeta_l + 1)} \right]}}{q\sqrt{2\pi c_2} \left[ \frac{3qr\overline{\gamma}_{b_i} + 2(M-1)(\zeta_l + 1)}{2(M-1)(\zeta_l + 1)} \right]^d} - \frac{2 \left(1 - \frac{1}{\sqrt{M}}\right)^2 \cdot e^{-d \cdot \zeta \left[ \frac{3qr\overline{\gamma}_{b_i}}{3qr\overline{\gamma}_{b_i} + 2(M-1)(\zeta_l + 1)} \right]}}{\pi c_2 q \left[ \frac{3qr\overline{\gamma}_{b_i} + (M-1)(\zeta_l + 1)}{(M-1)(\zeta_l + 1)} \right]} \tag{5}$$



where  $c_2 = 2.6 + 0.1\zeta$  is empirically obtained and  $d=1$  for HDD.  $\zeta_i$  is the ratio of direct-to-diffuse signal power on the  $i^{th}$  sub-channel.  $\zeta$  has 0 in a pure Rayleigh fading channel and ranges from 0 to 10 in a composite Rayleigh/Ricean fading channel.  $\overline{\gamma_{bi}}$  is the ratio of received average energy per bit-to-noise power spectral density on the  $i^{th}$  sub-channel. The overall  $p$  is the average of the probability of bit error on each of the  $N$  OFDM sub-channels.

$$p = \frac{1}{N} \sum_{i=1}^N p_i \tag{6}$$

Note that for either no channel fading or for all sub-channels experiencing the same fading (that is,  $\zeta_i = \zeta$  and  $\overline{\gamma_{bi}} = \overline{\gamma_b}$  for all  $i$ ), then  $p_i = p \cdot \overline{\gamma_b} = \overline{E_b} / N_o$  is the ratio of received average energy per bit-to-noise power spectral density,  $\zeta$  is the ratio of direct-to-diffuse signal power. Now, using equation (6) in equation (3) or (4) and taking the result into equation (2), we obtain the performance of 64 QAM with HDD over Ricean fading channels. For basic access mechanism, a data packet including the PHY header and the MAC header needs retransmission if any one bit of them is corrupted. We define a variable  $P_C$  which is the probability that a backoff occurs in a station due to bit errors in frames. We further assume that bit errors randomly appear in the frames. So frame error rate is represented by (7).

$$P_C = 1 - (1 - P_b)^{L_{preamble} + PHY_h + MAC_h + P + LACK} \tag{7}$$

CSMA/CA is also used as the MAC scheme in IEEE 802.11n wireless LAN, and it has basic and RTS/CTS access scheme. Although there is a successful RTS/CTS transmission in the time slot, a frame have to be retransmitted when there is a bit error in a payload. For convenience, we define a variable  $P_e$  which is the probability that a backoff occurs in a station due to bit errors in frames. We further assume that bit errors randomly appear in the frames and A-MSDU scheme is used. So frame error rate is represented by (8).

$$P_e = 1 - (1 - q)^L \tag{8}$$

Where  $L$  is the aggregated MAC frame's size. For a convolutional code with a coding rate  $k_c/n_c$ , the bit error rate, denoted as  $q$ , can be approximated by

$$q = \frac{1}{k_c} \sum_{i=\frac{d_{free}+1}{2}}^{d_{free}} \binom{d_{free}}{i} (q_b)^i (1 - q_b)^{d_{free}-i} \quad (d_{free} \text{ is odd}) \tag{9}$$

$$q = \frac{1}{k_c} \sum_{i=\frac{d_{free}}{2}+1}^{d_{free}} \binom{d_{free}}{i} (q_b)^i (1 - q_b)^{d_{free}-i} + \frac{1}{2k_c} \binom{d_{free}}{d_{free}/2} (q_b)^{d_{free}/2} (1 - q_b)^{d_{free}/2} \quad (d_{free} \text{ is even})$$

Where  $d_{free}$  is the maximum free distance of the convolutional code and  $q_b$  is the probability of a bit error for the M-QAM.

$$q_b = \frac{Mq_s}{2(M-1)} \quad (10)$$

$q_s$  is the SER(Symbol Error Rate) under the Rician fading channel.

$$q_s = \left( \frac{1+K}{1+K + \frac{\rho(d_{\min})^2}{8}} \right)^4 e^{-4} \left( \frac{\frac{\rho(d_{\min})^2}{8} (|H|^2)}{1+K + \frac{\rho(d_{\min})^2}{8}} \right) \quad (11)$$

$K$  is the Rician factor and  $\rho$  may be interpreted as the average SNR at the receive antenna in a SISO fading link.  $d_{\min}$  is the minimum distance of separation of the underlying scalar constellation.  $H$  is  $M_R \times M_T$  channel transfer function and  $\|H\|^2$  is the squared Frobenius norm of the channel.

### 5.1.2 Frame error rate of mobile wireless channel

Mobile wireless channel is assumed to be flat fading Rayleigh channel with Jake spectrum. The channel is in fading states or inter-fading states by evaluating a certain threshold value of received signal power level. If and only if the whole frame is in inter-fading state, there is the successful frame transmission. If any part of frame is in fading duration, the frame is received in error. In the fading channel fading margin is considered and defined as  $\rho = R_{req}/R_{rms}$ . Where  $R_{req}$  is the required received power level and  $R_{rms}$  is the mean received power. Generally, the fading duration and inter-fading duration can be taken to be exponentially distributed for  $\rho < -10$ dB. With the above assumptions, let  $T_{pi}$  be the frame duration, then the frame error rate is given by (12).

$$FER = 1 - \frac{T_i}{T_i + T_f} P(t_i > T_{pi}) \quad (12)$$

Where,  $t_i$  is inter-fading duration and  $t_f$  is fading duration.  $T_i$  is the mean value of the random variable  $t_i$  and  $T_f$  is the mean value of the random variable  $t_f$ .  $P(t_i > T_{pi})$  is the probability that inter-fading duration lasts longer than  $T_{pi}$ . Since exponential distribution is assumed for  $t_i$ ,  $P(t_i > T_{pi}) = \exp(-\frac{T_{pi}}{T_i})$ . For Rayleigh fading channel, the average fading duration is given by (13).

$$T_i = \frac{\exp(\rho) - 1}{f_d \sqrt{2\pi\rho}} \quad (13)$$

$T_i + T_f$  is  $\frac{1}{N_f}$ , where  $N_f$  is the level crossing rate, which is given by  $f_d \sqrt{2\pi\rho} \exp(-\rho)$ .  $f_d$  is the maximum Doppler frequency and evaluated as  $\frac{v}{\lambda}$ .  $v$  is the mobile speed and  $\lambda$  is wavelength. Frame error rate can be expressed by (14) [11].

$$FER = 1 - \exp(-\rho - f_d \sqrt{2\pi\rho} T_{pi}) \quad (14)$$

Equation (14) shows that frame error rate is determined by fading margin, maximum Doppler frequency and frame duration. Since fading margin and maximum Doppler frequency are hard to dynamically control, the only controllable parameter is frame duration to get required frame error rate. For the RTS/CTS access mode, the frame duration  $T_{pi}$  is  $T_H + T_{RTS} + T_{CTS} + T_{DATA} + T_{ACK}$ .  $T_H$  is preamble transmission time + PLCP header transmission time + MAC header transmission time.  $T_{DATA}$  is MSDU transmission time and  $T_{ACK}$  is ACK frame transmission time.  $T_{RTS}$  is RTS frame transmission time and  $T_{CTS}$  is CTS frame transmission time.

## 5.1.3 Numerical results

### 5.1.3.1 Analysis of frame error rate under the Rayleigh/Rician fading channel with fixed stations

In the Fig. 15,  $P_c(P, \gamma_b, K)$  shows PER(Packet Error Rate) due to  $\gamma_b$ , the ratio of received average energy per bit-to-noise power spectral density.  $K$  means Rician factor and  $P$  means payload size. and as expected, the PER (Frame Error Rate) performance improves with  $K$  and the smaller payload size is, the better performance is.

In the Fig. 16,  $q_s(\rho, K)$  shows SER(Symbol Error Rate) and  $P_c(K, \rho, n_s, P)$  shows PER(Packet Error Rate).  $K$  means Rician factor and as expected, the SER performance improves with  $K$ . Also, the PER performance improves with  $K$  and the smaller subframe' payload size is, the better performance is.

### 5.1.3.2 Analysis of frame error rate under the flat fading Rayleigh channel with mobile stations

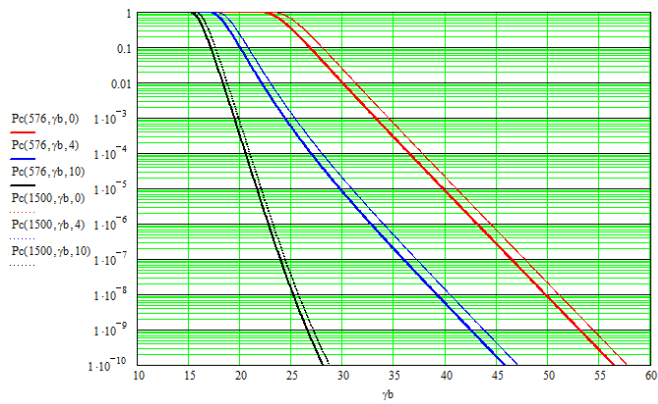
In the Fig. 17(a) ~ Fig. 17(c), the symbol  $fer(\rho, \nu, P)$  shows frame error rate of IEEE 802.11a/g. In the Fig. 17(d), the symbol  $fer(ns, \rho, \nu, P)$  shows frame error rate of IEEE 802.11n with the horizontal parameter of subframe' payload size. In the Fig. 17(e), the symbol  $fer(\rho, ns, \nu, P)$  shows frame error rate of IEEE 802.11n using the number of subframes as the horizontal parameter. It is generally identified that the higher mobile speed is, the higher frame error rate is. In case of payload size, the same result mentioned above is also acquired.

## 5.2 DCF throughput analysis

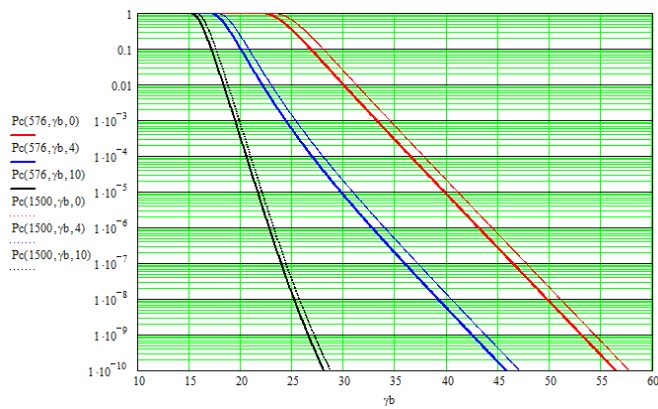
The back-off procedure of the DCF protocol is modeled as a discrete-time, two-dimensional Markov chain. Fig. 18 shows the Bianchi's Markov chain model for the back-off window size. We define  $W = CW_{\min}$ . Let  $m$ , the maximum back-off stage, be such value that

$CW_{\max} = 2^m W$ . We also define  $W_i = 2^i W$ , where  $i \in (0, m)$  is called the back-off stage. Let  $s(t)$  be the stochastic process representing the back-off stage  $(0, \dots, m)$  of the station at time  $t$ .  $p$  is the probability that a transmission is collided or unsuccessfully executed.

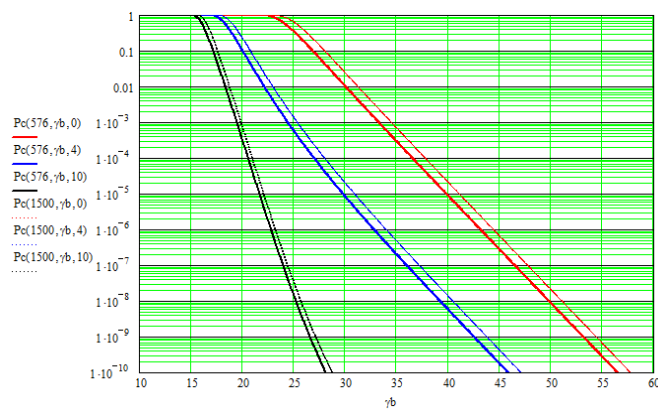
We will present the analytical evaluation of saturation throughput with bit errors appearing in the transmitting channel. The number of stations  $n$  is assumed to be fixed and each station always has packets for transmission. In other words, we operate in saturation conditions, the transmission queue of each station is assumed to be always nonempty.



(a) 802.11a OFDM

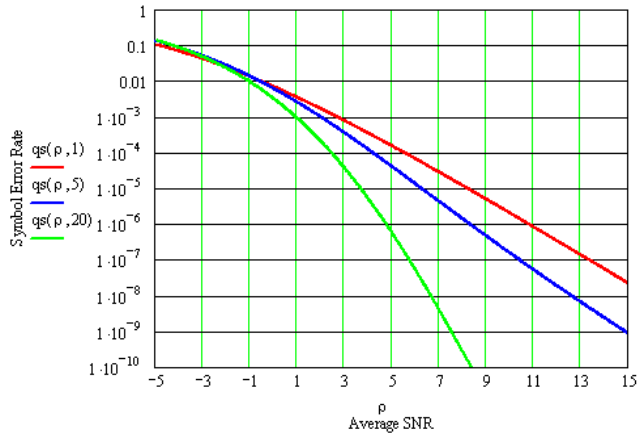


(b) 802.11g ERP-OFDM

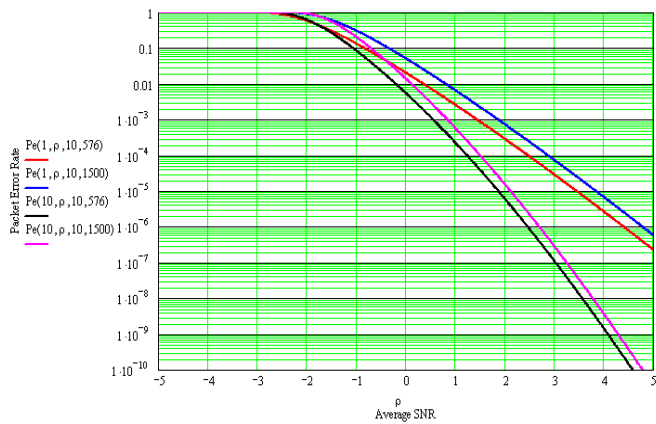


(c) 802.11g DSSS-OFDM

Fig. 15. Frame error rate of IEEE 802.11a/g fixed LAN over Rayleigh fading channel

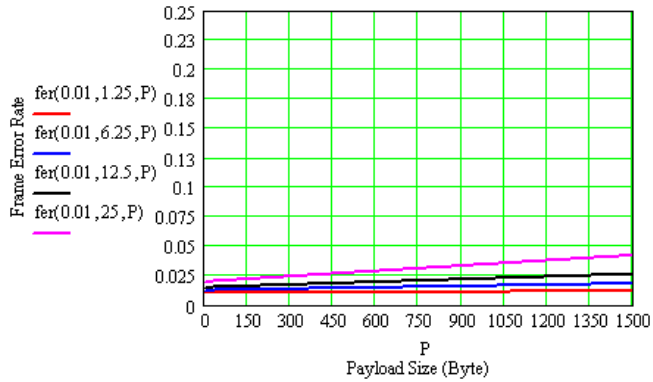


(a) Symbol error rate

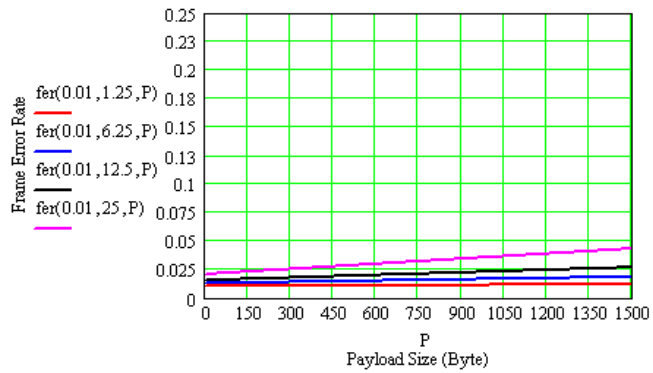


(b) Packet error rate

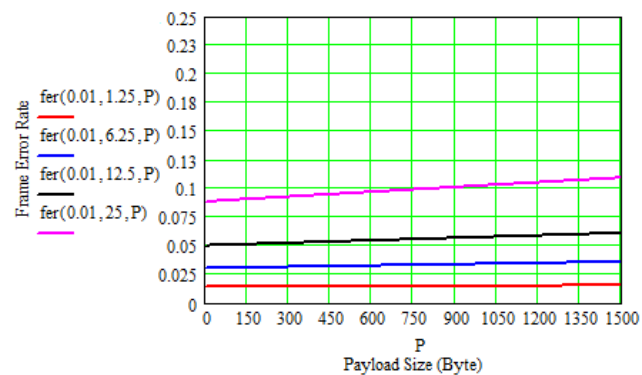
Fig. 16. Frame error rate of IEEE 802.11n fixed LAN over Rician fading channel



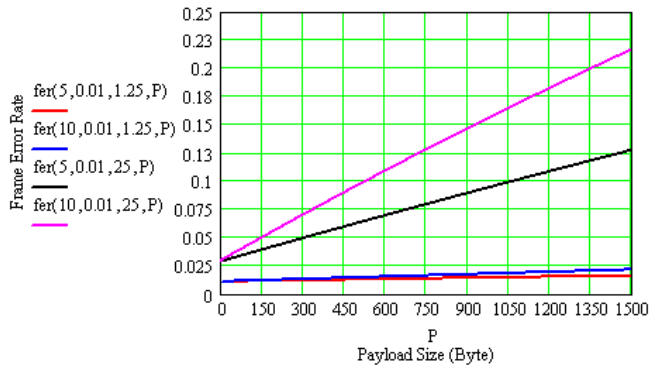
(a) 802.11a OFDM (54 Mbps)



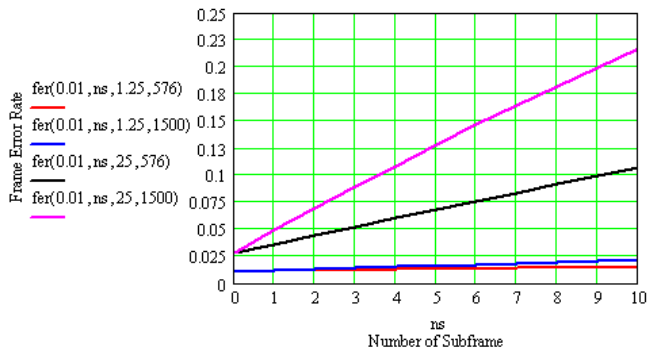
(b) 802.11g ERP-OFDM (54 Mbps)



(c) 802.11g DSSS-OFDM (54 Mbps)



(d) 802.11n OFDM (58.5 Mbps, Payload size)



(e) 802.11n OFDM (58.5 Mbps, number of subframe)

Fig. 17. Frame error rate of IEEE 802.11a/g/n mobile LAN

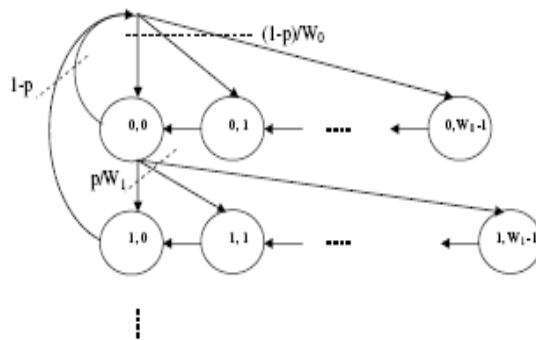


Fig. 18. Markov chain model for the backoff window size [20]

Let  $S$  be the normalized system throughput, defined as the fraction of time in which the channel is used to successfully transmit payload bits.  $P_r$  is the probability that there is at

least one transmission in the considered slot time. Since  $n$  stations contend on the channel and each transmits with probability  $\tau$ , we get

$$P_{tr} = 1 - (1 - \tau)^n \quad (15)$$

Table 12 shows physical and MAC layer parameters of IEEE 802.11a/g/n-based wireless LAN [21].

Parameter	Explanation
FER	Frame error rate
$\tau$	Packet transmission probability
$n$	Number of stations
$P$	Payload size
$T_{RTS}$	RTS frame transmission time
$T_{CTS}$	CTS frame transmission time
$T_H$	PLCP preamble transmission time + PLCP header transmission time + MAC header transmission time
$T_{DATA}$	Payload transmission time
$T_{ACK}$	ACK frame transmission time
$T_{BACK}$	Block ACK frame transmission time
$\sigma$	Slot time
$T_{SIFS}$	SIFS time
$T_{DIFS}$	DIFS time
$T_{EIFS}$	EIFS time
$CW_{min}$	Minimum backoff window size
$CW_{max}$	Maximum backoff window size

Table 12. IEEE 802.11a/g/n PARAMETERS

### 5.2.1 IEEE 802.11a/g DCF throughput

Saturation throughput is represented as shown in (16)[5].

$$S = \frac{P_s P_{tr} P}{(1 - P_{tr})\sigma + P_{tr} P_s T_s + P_{tr} (1 - P_s) T_c} = \frac{n\tau(1 - \tau)^{n-1}(1 - FER)P}{(1 - \tau)^n \sigma + n\tau(1 - \tau)^{n-1}(1 - FER)T_s + [1 - (1 - \tau)^n]T_c - n\tau(1 - \tau)^{n-1}(1 - FER)T_c} \quad (16)$$

$P_s$  is the probability that a transmission successfully occurs on the channel and is given by the probability that exactly one station transmits on the channel, conditioned on the fact that at least one station transmits.

$$P_s = \frac{n\tau(1 - \tau)^{n-1}(1 - FER)}{P_{tr}} \quad (17)$$



The average amount of payload information successfully transmitted in a slot time is  $P_{tr}P_sP$ , since a successful transmission occurs in a slot time with probability  $P_{tr}P_s$ . The average length of a slot time is readily obtained considering that, with probability  $1 - P_{tr}$ , the channel is empty, with probability  $P_{tr}P_s$  it contains a successful transmission, and with probability  $P_{tr}(1 - P_s)$  it contains a collision. Where  $T_s$  is the average time the channel is sensed busy because of a successful transmission, and  $T_c$  is the average time the channel is sensed busy by each station during a collision or error.  $\sigma$  is the duration of an empty slot time. In the RTS/CTS access scheme, we obtain,

$$T_s = T_{RTS} + T_{CTS} + T_{DATA} + T_{ACK} + T_{DIFS} + 3T_{SIFS} \tag{18}$$

$$T_c = T_{RTS} + T_{EIFS} = T_{RTS} + T_{SIFS} + T_{ACK} + T_{DIFS}$$

**5.2.2 IEEE 802.11n DCF throughput**

The saturation throughput can be calculated as follows [9].

$$S = \frac{E_p}{E_t} = \frac{L_p P_{tr} P_s (1 - P_e)}{T_{idle} P_{idle} + T_c P_{tr} (1 - P_s) + T_e P_{err} + T_{succ} P_{succ}} = \frac{L_p n \tau (1 - \tau)^{n-1} (1 - P_e)}{(1 - \tau)^n \sigma + n \tau (1 - \tau)^{n-1} (1 - P_e) T_{succ} + [1 - (1 - \tau)^n - n \tau (1 - \tau)^{n-1}] T_c + n \tau (1 - \tau)^{n-1} P_e T_e} \tag{19}$$

where  $E_p$  is the number of payload information bits successfully transmitted in a virtual time slot, and  $E_t$  is the expected length of a virtual time slot.  $P_e$  is the error probability on condition that there is a successful RTS/CTS transmission in the time slot.  $P_{idle}$  is the probability of an idle slot.  $P_s$  is the probability for a non-collided transmission.  $P_{err}$  is the transmission failure probability due to error (no collisions but having transmission errors).  $P_{succ}$  is the probability for a successful transmission without collisions and transmission errors.  $T_{idle}$ ,  $T_c$  and  $T_{succ}$  are the idle, collision and successful virtual time slot's length.  $T_e$  is the virtual time slot length for an error transmission sequence.  $L_p$  is the aggregated frame's payload length. In the RTS/CTS scheme, we obtain,

$$T_c = T_{RTS} + T_{EIFS} \tag{20}$$

$$T_{succ} = T_{RTS} + T_{CTS} + T_{DATA} + T_{BACK} + 3T_{SIFS} + T_{DIFS}$$

$$T_e = T_{RTS} + T_{CTS} + T_{DATA} + T_{EIFS} + 2T_{SIFS}$$

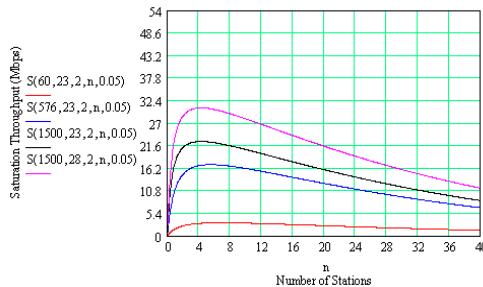
**5.2.3 Numerical results**

**5.2.3.1 Analysis of IEEE 802.11a/g/n DCF saturation throughput under the Rayleigh fading channel with fixed stations**

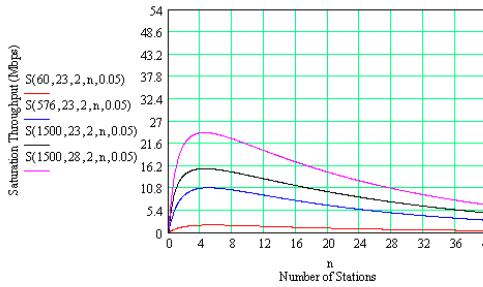
We analyze and compare the DCF throughput with the maximum physical transmission rate of 54 Mbps between IEEE 802.11a and 802.11g-based wireless Internet as shown in Fig. 19. Of the four different physical layers defined in the IEEE 802.11g standard, ERP-OFDM and DSSS-

OFDM are used. Three common packet sizes of 60 bytes(TCP ACK), 576 bytes(typical size for web browsing) and 1,500 bytes(the maximum size for Ethernet) are considered.

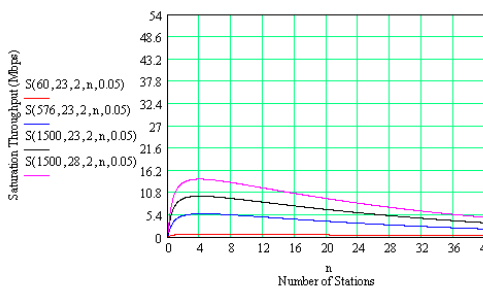
In the Fig.19,  $S(P, \gamma_b, \zeta, n, \tau)$  shows the saturation throughput over error-prone channel due to number of stations( $n$ ) for common packet sizes on the condition that packet transmission probability( $\tau$ ), average energy per bit-to-noise power spectral density( $\gamma_b$ ) and the ratio of direct-to-diffuse signal power( $\zeta$ ) are fixed.



(a) IEEE 802.11a



(b) IEEE 802.11g ERP-OFDM

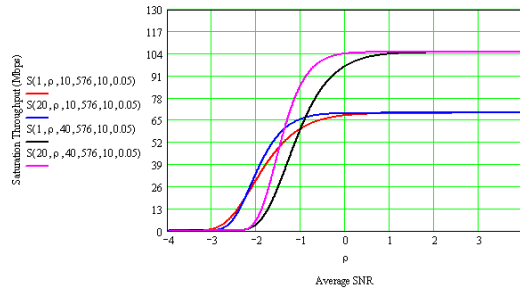


(c) IEEE 802.11g DSSS-OFDM

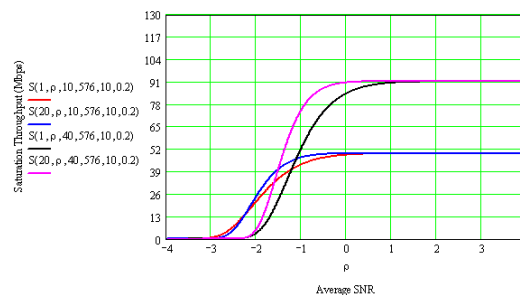
Fig. 19. DCF throughput in 802.11a/g ERP-OFDM/g DSSS-OFDM (54 Mbps)

The larger payload size be, the higher saturation throughput be for error-prone channel. It is identified that there are optimum number of stations corresponding to maximum saturation throughput. The DCF saturation throughput of 802.11a is the highest for error-prone channel. Because system needs 25 dB minimum signal to noise ratio at the data rate of 54 Mbps, this paper used 23 dB and 28 dB as the signal to noise ratio.

We evaluated DCF throughput performance of IEEE 802.11n wireless LAN based on MIMO OFDM with the system parameter defined in Table 12. MCS (Modulation and Coding Scheme) index 15 is used to generate the physical data rate of 130 Mbps with 20 MHz bandwidth and long guard interval. And the two common packets passed down to the MAC layer are 576 bytes (typical size for web browsing) and 1,500 bytes (the maximum size for Ethernet) in length.  $S(K, \rho, n_s, P, n, \tau)$  shows DCF throughput performance over the Rician fading channel. Fig. 20(a) shows DCF throughput on the condition that the subframe' payload size is 576 bytes, the number of stations is 10 and the packet transmission probability is 0.05. In that Fig. 20(a), it is identified most of the the ratio of received average energy per bit-to-noise power spectral density that the larger the Rician factor and the number of subframe are, the better the DCF throughput performance is. Fig. 20(b) has the same condition as Fig 20(a) except the packet transmission probability 0.05 replaced by 0.2. It is identified that if the packet transmission probability is lower, the DCF throughput performance is improved because packet collision probability is decreased. Fig 20(c) has the same condition as Fig. 20(a) except the number of stations 10 replaced by 30. Fig 20(d) is compared to Fig 20(a) about the DCF throughput performance for the subframe size, 576 bytes and 1,500 bytes. It is identified that the larger the subframe' payload size is, the better the DCF throughput performance is.



(a) P=576 bytes, n=10,  $\tau=0.05$



(b) P=576 bytes, n=10,  $\tau=0.2$

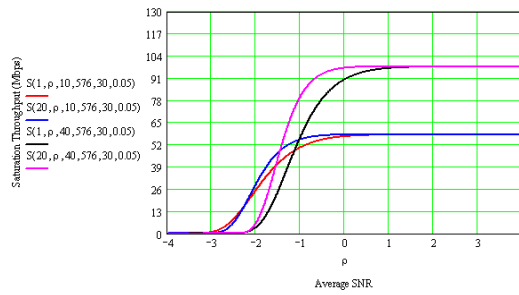
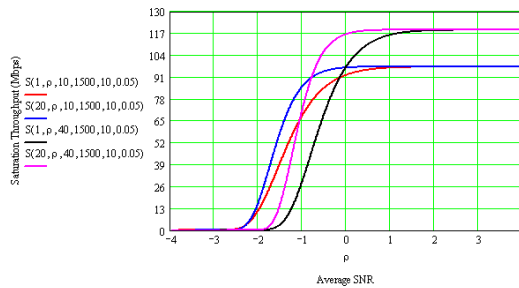
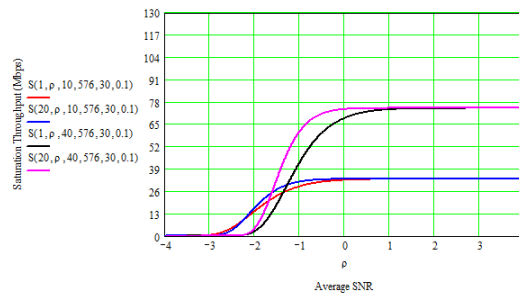
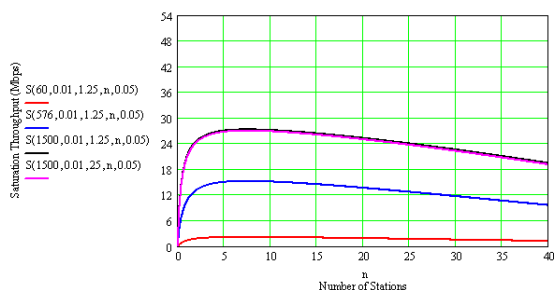
(c)  $P=576$  bytes,  $n=30$ ,  $\tau=0.05$ (d)  $P=1,500$  bytes,  $n=10$ ,  $\tau=0.05$ (e)  $P=576$  bytes,  $n=30$ ,  $\tau=0.1$ 

Fig. 20. DCF throughput in 802.11n (130 Mbps)

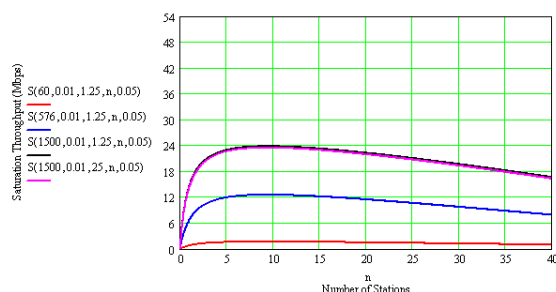
### 5.2.3.2 Analysis of IEEE 802.11a/g/n DCF saturation throughput under flat Rayleigh fading channel with mobile station

This section evaluated DCF throughput of the IEEE 802.11a/g-based mobile LAN with the maximum physical transmission rate of 54 Mbps and that of the IEEE 802.11n-based mobile LAN with the physical transmission rate of 130 Mbps considering 20 MHz MCS (modulation and coding scheme) parameters for two spatial streams, as shown in Fig. 21. Out of the four different physical layers defined in the IEEE 802.11g standard, both ERP-OFDM and DSSS-OFDM standard are only used owing to their maximum transmission rate of 54 Mbps in this evaluation. And the three common packets passed down to the MAC layer are 60 bytes (TCP ACK), 576 bytes (typical size for web browsing) and 1,500 bytes (the maximum size for

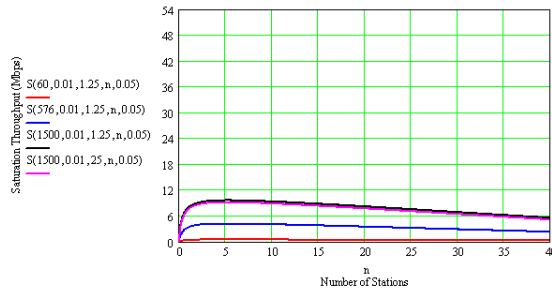
Ethernet) in length. In the IEEE 802.11n-based mobile LAN, the number of packets aggregated in one MAC frame varies from 1 to 100, which leads to an aggregated frame's payload length ( $L_p$ ) from 60, 576 and 1,500 bytes to 6, 57.6 and 150 Kbytes. In the Fig. 21(a) ~ Fig. 21(c), the symbol  $S(P, \rho, \nu, n, \tau)$  shows the saturation throughput over error-prone channel according to the number of stations( $n$ ) for common packet sizes ( $P$ ) on the condition that packet transmission probability ( $\tau$ ), mobile velocity ( $\nu$ ) and fading margin ( $\rho$ ) are fixed. In the Fig. 21(d) and Fig. 21(e), the symbol  $S(ns, P, \rho, \nu, n, \tau)$  and  $S(P, ns, \rho, \nu, n, \tau)$  respectively shows the saturation throughput over error-prone channel according to the number of stations ( $n$ ) and the typical number of packets aggregated in one MAC frame ( $ns$ ) for two subframe length on the condition that packet transmission probability ( $\tau$ ), mobile velocity ( $\nu$ ) and fading margin( $\rho$ ) are fixed. For example, in the Fig. 21(a), if the number of stations is 7, packet transmission probability is 0.05, packet length is 1,500 and fading margin is 0.01, mobile station with the speed of 1.25 m/s can get the throughput of 27.238 Mbps, whereas mobile station with the speed of 25 m/s can get the throughput of 26.968 Mbps. In the Fig. 21(d), if subframe length is 30 and the same conditions mentioned above are applied, mobile station with the speed of 1.25 m/s can get the throughput of 113.511 Mbps with six stations, whereas mobile station with the speed of 25 m/s can get the throughput of 84.607 Mbps. Also, Fig. 21(a ~ d) shows that the longer frame (or subframe) length is, the higher throughput is. And, for the same frame (or subframe) length, the higher speed is, the lower throughput is. As the results of evaluation, we also know that there is optimum number of stations to maximize saturation throughput under the error-prone channel. Specially, in Fig 21(e), the number of subframes is considered and it is identified that there is optimum number of subframes to maximize saturation throughput under the error-prone channel.



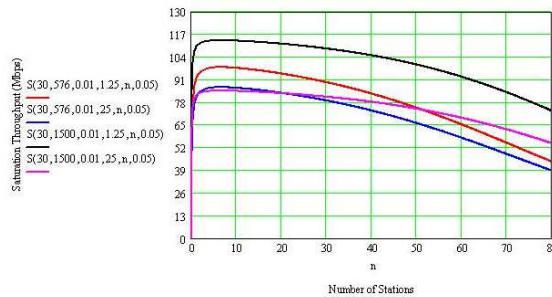
(a) 802.11a OFDM (54 Mbps)



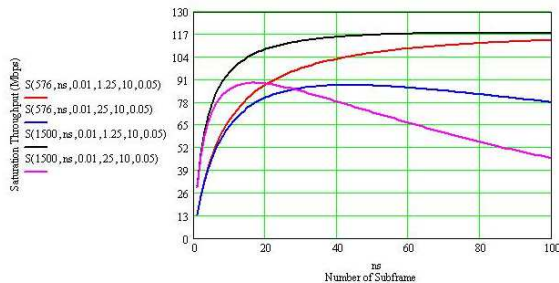
(b) 802.11g ERP-OFDM (54 Mbps)



(c) 802.11g DSSS-OFDM (54 Mbps)



(d) 802.11n OFDM (130 Mbps, number of stations)



(e) 802.11n OFDM (130 Mbps, number of subframe)

Fig. 21. DCF throughput of IEEE 802.11a/g/n mobile LAN[12, 22]

In conclusion, we obtained the fact that there exist an optimal number of stations (or subframes) to maximize the saturation throughput under the error-prone channel. Also, we can identify that the larger payload (or subpayload) size be, the higher saturation throughput be. And if a mobile velocity of station is increased, the throughput is decreased a little. Out of the three different physical layers defined in this analysis with the maximum transmission rate of 54 Mbps, which are 802.11g ERP-OFDM, 802.11g DSSS-OFDM and 802.11a OFDM, The DCF saturation throughput of 802.11a OFDM is the highest at all the channel environments. In the case of 802.11n, because A-MSDU scheme is applied, it is identified that MAC efficiency of IEEE 802.11n is the best out of all four schemes.

## 6. Remarks

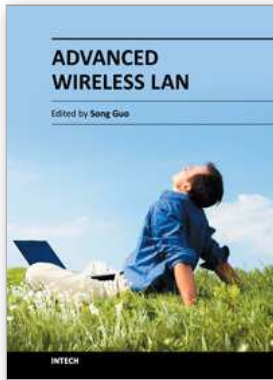
This chapter explored the saturation throughput performance of DCF protocol in the IEEE 802.11a/g/n-based fixed and mobile LAN under the error-prone channel. IEEE 802.11a and IEEE 802.11g have the same maximum transmission rate of 54 Mbps, but the DCF saturation throughput of 802.11a is higher than that of 802.11g. Of the two 802.11g standards, DCF saturation throughput of 802.11g ERP-OFDM is higher than that of 802.11g DSSS-OFDM. We are recognizing that a 802.11n-based device can operate with a 802.11 legacy devices, but 802.11a-based device does not operate with a 802.11b/g-based device. So either constructing 802.11a/n-based mobile LAN or constructing 802.11g/n-based mobile LAN have to be considered for interoperability.

## 7. References

- [1] Upkar Varshney, "The Status and Future of 802.11-based Wireless LANs," *IEEE Computer*, Jun. 2003, pp. 102-105.
- [2] Guido R. Hiertz, Dee Denteneer, Lothar Stibor, Yunpeng Zang, Xavier Pérez Costa and Bernhard Walke, "The IEEE 802.11 Universe," *IEEE Communications Magazine*, January 2010, pp. 62-70
- [3] Sixto Ortiz Jr., "IEEE 802.11n: The Road Ahead," *IEEE Computer*, July 2009, pp. 13-15
- [4] Eldad Perahia, "IEEE 802.11n Development: History, Process, and Technology," *IEEE Communications Magazine*, Jul. 2008, pp.48-55
- [5] Zuoyin Tang, Zongkai Yang, Jianhua He, and Yanwei Liu, "Impact of Bit Errors on the Performance of DCF for Wireless LAN," *IEEE*, 2002, pp. 529-533.
- [6] Yang Xiao and Jon Rosdahl, "Throughput and Delay Limits of IEEE 802.11," *IEEE Communications Letters*, Vol. 6, No. 8, August 2002, pp. 355 - 357
- [7] Jangeun Jun, Pushkin Peddabachagari and Mihail Sichitiu, "Theoretical Maximum Throughput of IEEE 802.11 and its Applications," *Proceedings of the Second IEEE International Symposium on Network Computing and Applications (NCA'03)*, 2003.
- [8] Dimitris Vassis, George Kormentzas, Angelos Rouskas, and Ilias Maglogiannis, "The IEEE 802.11g Standard for High data rate WLANs," *IEEE Network*, May/June. 2005, pp. 21-26.
- [9] Y. Lin and V. W. S. Wong, "Frame Aggregation and Optimal Frame Size Adaptation for IEEE 802.11n WLANs," in *Proc. IEEE GLOBECOM*, San Francisco, CA, Nov. 2006
- [10] D.Skordoulis, Q.Ni, H.Chen,A.P.Stephens, C.Liu, and A.Jamalipour, "IEEE 802.11n MAC Frame Aggregation Mechanisms for Next-Generation High-Throughput WLANs," *IEEE Wireless Communications*, vol.15, Feb. 2008, pp. 40-47.
- [11] Xi Yong, Wei Ji Bo, and Zhuang Zhao Wen, "Throughput Analysis of IEEE 802.11 DCF over Correlated Fading Channel in MANET," *IEEE*, 2005, pp. 694-697.
- [12] Ha Cheol Lee, "A MAC Layer Throughput over Error-Free and Error-Prone Channel in The 802.11a/g-based Mobile LAN," *MICC 2009*, Dec. 2009
- [13] Jeff Smith, Jake Woodhams and Robert Marg, "Controller-Based Wireless LAN Fundamentals," Cisco Press, 2011, pp. 71-72
- [14] Eldad Perahia and Robert Stacey, "Next Generation Wireless LANs," Cambridge University Press, 2008, pp. 130

- [15] Thomas Paul and Tokunbo Ogunfunmi, "Wireless LAN Comes of Age: Understanding the IEEE 802.11n Amendment," *IEEE Circuits and Systems Magazine*, First Quarter 2008, pp. 28-54
- [16] Wireless Gigabit Alliance, "WiGig White Paper: Defining the Future of Multi-Gigabit Wireless Communications, July 2010, pp. 2-5
- [17] Ryuta Imashioya, Wahyul Amien Syaifei, Yuhei Nagao, Masayuki Kurosaki, Baiko SAI and Hiroshi Ochi, "RTL Design of 1.2Gbps MIMO WLAN System and Its Business Aspect," *ISCIT 2009*, pp. 296-301
- [18] Chang Soon Choi, Eckhard Grass and Maxim Piz, "Performance Evaluation of Gbps OFDM PHY Layers for 60-GHz Wireless LAN Applications," *IEEE Conference*, 2009.
- [19] Chi-han Kao, "Performance of the IEEE 802.11a Wireless LAN Standard over Frequency-selective, Slow, Ricean Fading Channels," *Master's Thesis*, Sep. 2002.
- [20] Giuseppe Bianchi, "Performance Analysis of the IEEE 802.11 Distributed Coordination Function," *IEEE Journal on Selected Areas in Communications*, Vol. 18, No.3, pp. 535-547, Mar. 2000.
- [21] IEEE Std 802.11n 2009 " Part11: Wireless LAN Medium Access Control(MAC) and Physical Layer (PHY) specifications: Enhancements for Higher Throughput," Oct. 2009.
- [22] Ha Cheol Lee, "A MAC Throughput over Rayleigh Fading Channel in The 802.11a/g/n-based Mobile LAN," *MESH 2011*, Aug. 2011





## **Advanced Wireless LAN**

Edited by Dr. Song Guo

ISBN 978-953-51-0645-6

Hard cover, 136 pages

**Publisher** InTech

**Published online** 05, June, 2012

**Published in print edition** June, 2012

The past two decades have witnessed startling advances in wireless LAN technologies that were stimulated by its increasing popularity in the home due to ease of installation, and in commercial complexes offering wireless access to their customers. This book presents some of the latest development status of wireless LAN, covering the topics on physical layer, MAC layer, QoS and systems. It provides an opportunity for both practitioners and researchers to explore the problems that arise in the rapidly developed technologies in wireless LAN.

### **How to reference**

In order to correctly reference this scholarly work, feel free to copy and paste the following:

Ha Cheol Lee (2012). A MAC Throughput in the Wireless LAN, Advanced Wireless LAN, Dr. Song Guo (Ed.), ISBN: 978-953-51-0645-6, InTech, Available from: <http://www.intechopen.com/books/advanced-wireless-lan/a-mac-throughput-in-the-wireless-lan>

**INTECH**  
open science | open minds

### **InTech Europe**

University Campus STeP Ri  
Slavka Krautzeka 83/A  
51000 Rijeka, Croatia  
Phone: +385 (51) 770 447  
Fax: +385 (51) 686 166  
[www.intechopen.com](http://www.intechopen.com)

### **InTech China**

Unit 405, Office Block, Hotel Equatorial Shanghai  
No.65, Yan An Road (West), Shanghai, 200040, China  
中国上海市延安西路65号上海国际贵都大饭店办公楼405单元  
Phone: +86-21-62489820  
Fax: +86-21-62489821

© 2012 The Author(s). Licensee IntechOpen. This is an open access article distributed under the terms of the [Creative Commons Attribution 3.0 License](#), which permits unrestricted use, distribution, and reproduction in any medium, provided the original work is properly cited.